PATHOLOGICAL STUDIES ON THE HISTOGENESIS OF MALIGNANT FIBROUS HISTIOCYTOMA IN THE RAT

ラットの悪性線維性組織球腫の組織発生に関する病理学的研究

JYOJI YAMATE

(1)

PATHOLOGICAL STUDIES ON THE HISTOGENESIS OF MALIGNANT FIBROUS HISTIOCYTOMA IN THE RAT

JYOJI YAMATE

CONTENTS

PREFACE

Malignant fibrous histiocytoma (MFH), also called previously malignant fibrous xanthoma or fibroxanthosarcoma, was first described as a new entity of soft-tissue tumor in humans by O'Brien and Stout in 1964. Since then MFH has been reported to be the most common neoplasm of the soft-tissue in the elderly (Enjoji et al., 1980; Stiller and Katenkamp, 1981). MFH in humans arises mainly in the limbs, especially in the leg and thigh, and occasional cases have been found in the lungs (Tanino et al., 1985), gastrointestinal tract (Satake and Matsuyama, 1988; Shibuya et al., 1985), uterus (Takaki et al., 1983), bone (Stiller and Katenkamp, 1983) and nasal cavity (Tanaka, T. et al., 1982). On the contrary, spontaneous MFH in animals has rarely been detected in cats (Garma-Aviña, 1987; Gleiser et al., 1979; Renlund and Pritzker, 1984), dogs (Gleiser et al., 1979), pig (Tanimoto et al., 1988), primates (Gleiser and Carey, 1983; Skavlen et al., 1988), fox (Fujimaki et al., 1985), rabbit (Yamamoto and Fujishiro, 1989) and rats (Greaves et al., 1982; Maekawa et al., 1983; Solleveld et al., 1984; Ward et al., 1981). However, soft-tissue

tumors resembling human MFH have been experimentally induced in rats by agents such as 4-(hydroxyamino) quinoline 1-oxide (Konishi et al., 1982; Maruyama et al., 1983), nickel sulphide (Shibata et al., 1989), 9,10-dimethyl-1,2-benzanthracene (Kato et al., 1990), and millipore filters (Greaves et al., 1985).

MFH consists mainly of fibroblastic and histiocytic cells in various proportions and is often mixed with pleomorphic giant cells, xanthoma cells, and varying amounts of inflammatory cells. MFH is different histologically from other soft-tissue tumors such as liposarcoma, leiomyosarcoma, rhabdomyosarcoma, osteosarcoma, and fibrosarcoma in that MFH is characterized by neoplastic cells positive for lysosomal enzymes such as acid phosphatase and nonspecific esterase, often arranging in a storiform pattern. But MFH reveals a great variety of histologic appearances. Human MFH has been divided into the storiform, pleomorphic, myxoid, giant cell, and xanthogranulomatous (inflammatory) types (Enjoji et al., 1980; Stiller and Katenkamp, 1981). The storiform type consists of spindle cells arranged in a short fascicle or storiform pattern. The spindle cells are well differentiated and resemble fibroblasts.

Histiocytic cells are occasionally mixed with the spindle cells, and the stroma of this type contains a large amount of collagenic fibers encircling the spindle cells. Tumors consisting of spindle-shaped fibroblastic cells and greater numbers of rounded histiocytic cells arranged haphazardly without any particular growth patterns are referred to as the pleomorphic type. Cellular pleomorphism is usually more prominent in this type. Because a transition from storiform areas to pleomorphic areas has frequently been observed in MFH, some investigators have classified such tumors as the pleomorphic-storiform type, which is the most common variant of human MFH (Enjoji et al., 1980). The myxoid type is characterized by loosely arranged fibroblastic and histiocytic cells supported by alcian blue-positive myxomatous matrix. Although myxoid areas have occasionally been observed in the storiform and pleomorphic types, tumors, in which more than one-half of their cut-surface is occupied by myxoid areas, have been classified as this form. The giant cell type, also termed malignant giant cell tumor of soft part, is a tumor composed of a mixture of histiocytic cells, fibroblastic cells, and pleomorphic, multinucleated giant cells. The

hallmark of this type is an appearance of many giant cells. Although these giant cells resemble osteoclasts, it has been considered that they develop by fusion or amitotic division of histiocytic mononuclear cells. The inflammatory type consists of sheets of histiocytic cells and inflammatory cells supported by a stroma including a small amount of collagenic fibers. The majority of histiocytic cells appear xanthomatous because they contain lipid droplets in their cytoplasm. Occasional cases of this type develop granulation tissues consisting of xanthomatous cells and varying numbers of inflammatory cells, giving an appearance of xanthogranuloma. Besides aforementioned five variants, the angiomatoid form of MFH has recently been described in very young persons (Kay, 1985). This type is rare and less aggressive, and characterized by sheets of histiocytic cells intimately associated with blood-filled cystic spaces, intense inflammation, and extensive fibrosis, accompanied with multiple hemorrhages in the tumor tissues. The majority of spontaneous MFH hitherto reported in animals have been diagnosed as the storiform or pleomorphic type, except one feline case that was described as the giant cell type (Garma-Aviña, 1987).

The cellular origin of MFH remains undetermined, although histiocyte, fibroblast or undifferentiated cell has been proposed as a possible progenitor cell of MFH. Histochemical studies confirmed that neoplastic cells forming MFH reacted positively to lysosomal enzymes of histiocytes (Enjoji et al., 1980; Greaves et al., 1985; Nakanishi and Hizawa, 1984). In tissue culture studies, cells cultivated from human MFH were demonstrated to show functional and immunocytochemical characteristics of histiocytes (Inoue et al., 1984; Iwasaki et al., 1982; Shirasuna et al., 1985). Tumors resembling human MFH have been experimentally produced in mice by transplanting mouse bone marrow macrophages or peritoneal macrophages transformed with SV 40 (Hagari and Yumoto, 1987; Yumoto and Morimoto, 1980). Thus it has been considered that MFH may be derived from histiocytes, and that neoplastic histiocytes may be able to behave as facultative fibroblasts under appropriate conditions. Moreover, proliferating cells of human MFH have been found to react with monoclonal antibodies against determinants expressed on monocyte-macrophages, suggesting that MFH is a tumor of the mononuclear phagocyte system (Strauchen and Dimitriu-Bona, 1986). On the other hand, the storiform type

of MFH is characterized by frequent appearances of fibroblastic cells and a considerable amount of collagenic fibers. A human MFH-derived cell line has been reported to possess features of fibroblasts (Roholl et al., 1986). Krawisz et al. (1981) observed that mouse fibroblast-like cells differentiated into macrophages when cultivating them in a medium containing human serum. Fibroblasts have been known to be able to transform into histiocytes (Krawisk et al., 1981). Therefore, fibroblasts could be regarded as a possible progenitor cell of MFH. Ultrastructurally, primitive mesenchymal cells with poorly developed cytoplasmic organelles have occasionally been found in MFH, suggesting that both the histiocytic and fibroblastic cells constituting MFH may be derived from a common undifferentiated stem cell (Greaves et al., 1985; Maruyama et al., 1983; Roholl et al., 1985ab). It has recently been reported that xenografts of human MFH in nude mice expressed leiomyogenic or schwannian differentiation (Roholl et al., 1988), and that histologic phenotypes reminiscent of osteosarcoma, leiomyosarcoma, schwannoma, and liposarcoma were mixed in parts of human MFH (Brooks, 1986). These observations suggest that

MFH may be derived from a pluripotential mesenchymal cell. Hence it appears that the histogenesis of MFH is still controversial.

The present author established a transplantable tumor line from a spontaneous rat MFH in syngeneic rats. This line was designated MFH-MT. In an attempt to clarify the histogenesis of MFH, MFH-MT and *in vitro* passaged cells derived from MFH-MT were scrutinized in a series of studies. As a result, MFH-MT provided useful information on the histogenesis of MFH.

The first chapter describes morphologic characteristics of the original tumor and MFH-MT which was transplanted into syngeneic rats or heterotransplanted into nude mice. The second chapter mentions morphologic and functional characteristics of *in vitro* passaged cells (MT-P) derived from MFH-MT. In Chapter 3, glycosaminoglycans produced by neoplastic cells constituting MFH-MT were identified by histochemical stainings and cellulose acetate electrophoresis. In the fourth chapter, an antitumor drug (*cis*-Diamminedichloro-platinum)-selected cell line (MT-R10) was induced from MT-P, and its characteristics were investigated

in comparison with those of MT-P. To further clarify the properties of neoplastic cells constituting MFH, four cloned cell lines were established from MT-P. Characteristics of these cloned cell lines are described in the fifth chapter.

CHAPTER 1

MORPHOLOGIC CHARACTERISTICS OF A TRANSPLANTABLE TUMOR LINE (MFH-MT) DERIVED FROM A SPONTANEOUS RAT MALIGNANT FIBROUS HISTIOCYTOMA

INTRODUCTION

Malignant fibrous histiocytoma (MFH) is a sarcoma consisting of two main cells, fibroblastic and histiocytic cells, supported by collagenous or myxoid matrix and often arranged in a storiform pattern. Besides these cells, pleomorphic giant cells, xanthoma cells, and varying numbers of inflammatory cells are frequently mixed in MFH. Thus it has been well known that MFH shows highly variable histologic patterns (Enjoji et al., 1980; Stiller and Katenkamp, 1981). Based on the predominant cell types and the amount of intercellular material, human MFH has been classified into the storiform, pleomorphic, myxoid, xanthogranulomatous (inflammatory), and giant cell types (Enjoji et al., 1980).

Spontaneously occurring MFH has been detected in subcutaneous tissues of F344 rats used in life-span studies or in carcinogenicity tests as controls, ranging in incidence from 0.2 to 2.7% (Maekawa et al., 1983; Solleveld et al., 1984). In contrast to human MFH, no detailed descriptions have been given to these tumors. The present author succeeded in transplantation of a spontaneous MFH detected in a male F344 rat.

The transplantable tumor, designated MFH-MT, had been serially passaged up to the 45th generation in syngeneic rats. In this chapter, the original tumor and MFH-MT, which had been transplanted into syngeneic rats or heterotransplanted into nude mice, were morphologically examined. Furthermore, susceptibility of MFH-MT to antitumor drugs was investigated. These observations confirmed a wide range of histologic appearances of MFH-MT, as described in human MFH.

MATERIALS AND METHODS

Animals and Environment: Specific-pathogen-free male and female F344/DuCrj (F344) rats, which had been purchased from Charles River Japan, Inc. or produced in the author's laboratory, were used throughout the experiments. For heterotransplantation, athymic nude mice of 3 strains, BALB/c-nu/nu slc (Shizuoka Agricultural Cooperation Association), BALB/cA-Jcl-nu/nu (Clea Japan Inc.), and Crj:CD-1 (ICR)-nu/nu (Charles River Japan, Inc.), were used. The animals were maintaind in barrier rooms conditioned to a temperature of 23±2 ℃ and a relative humidity of 50±20%, and with a 12-hr light-dark cycle. A standard commercial laboratory diet for rats and mice (CRF-1: Charles River Japan, Inc.) and tap water were available ad libitum.

Serial Transplantation in Syngeneic Rats and Heterotransplantation in Athymic Nude Mice: Tumor masses were minced into small pieces, <2 mm in diameter, with scissors and then transplanted subcutaneously at the midline of the interscapular region through a trocar with a diameter of 2 mm.

The major (a) and minor (b) axes of tumors developing in subcutaneous tissue were measured once weekly with calipers and expressed by millimeter, and tumor volume was estimated by the following formula: $a \times b^2 / 2$.

The tumors were serially transplanted using two to four male and female F344 rats, 10 to 25 weeks of age, in each generation. The passage was repeated every 5 to 6 weeks after transplantation when tumor reached size of >5 cm in diameter. The growth curve of tumors in syngeneic rats was determined using ten 6-week-old male F344 rats, which were transplanted subcutaneously with a piece of tumor tissue from the 9th generation. Six of them were killed 6 weeks after transplantation, and the remainder were observed until death.

A histologic comparison was made between tumors transplanted at different sites of rat's body, since MFH has generally been known to be composed of different cell types and of variable histologic patterns depending on different portions of the tumors examined. Tumor tissues at the 4th and 11th passage levels were minced and trypsinized to disperse cells. After being washed in phosphate-buffered saline (PBS), 0.1 to 0.5 ml of a cell suspension containing 10^5 to

10^7 cells/ml were inoculated subcutaneously in the back and head, intraperitoneally, intradermally at the root of the tail, or intravenously.

Tumor growths in heterotransplantation were observed for 5 weeks in 5 male and 5 female nude mice for each of the 3 strains. These mice were transplanted subcutaneously with a piece of tumor tissue from the 21st generation at the age of 5 weeks.

Susceptibility of MFH-MT to Antitumor Drugs:
Adriamycin (ADR) obtained from Kyowa Hakko Kogyo Co., Ltd. (Tokyo, Japan) and cis-Diamminedichloroplatinum (CDDP) from Nippon Kayaku Co., Ltd. (Tokyo, Japan) were used as antitumor drugs. Experiments were performed on eighteen 6-week-old male rats which had been transplanted subcutaneously with a piece of tumor tissue from the 10th generation. The animals were allotted to 3 groups of 6 each; two groups were treated with the drugs and one group received distilled water via peritoneal route and served as controls. The antitumor drugs were injected intraperitoneally at dosage levels of 4 mg/kg for ADR and 5 mg/kg for CDDP, equivalent

to 1/4 and 2/3 of the 50% lethal doses by peritoneal route, respectively. The drugs were first injected on the following day after transplantation and thereafter, once weekly for 5 weeks.

Light Microscopy: Necropsies were performed on all the animals which were killed under anesthesia or found dead during the experiments. After being weighed, tumor tissues were fixed in 10% neutral buffered formalin. They were embedded in paraffin, sectioned, and stained with hematoxylin and eosin (HE). Selected sections were also stained with periodic acid-Schiff (PAS) with and without diastase digestion, Watanabe's silver impregnation for reticulin, azan-Mallory, alcian blue (pH 2.5) and by the von Kossa's method. Frozen sections from the formalin-fixed tissues were stained with Sudan Ⅲ and oil red O.

For enzyme histochemistry, fresh specimens were fixed in 4% formol calcium for 12 hr at 4 ℃, and stored in Holt's hypertonic gum sucrose solution for 12 to 24 hr. The tissues were frozen, and sections were cut at 10 μm thick and staind by the Gomori's method for acid phosphatase (ACP)(pH 5.0), by the

alpha-naphthyl acetate method for nonspecific esterase (NSE)(pH 7.4), and by the naphthol AS method for alkaline phosphatase (ALP)(pH 9.0).

Paraffin-embedded sections were immunohistochemically stained by the peroxidase-antiperoxidase (PAP) technique using a commercial kit (Cambridge Research Laboratory (CRL) Universal Immunoperoxidase Staining Kit, CRL, MA). Rabbit antisera to alpha-1 antitrypsin (CRL), S-100 protein (CRL), factor VIII-related antigen (CRL), myoglobin (CRL), lysozyme (CRL), keratin (CRL), and desmin (Miles Laboratory, Naperville, IL) were used as primary antibodies. Normal rabbit sera were used as negative controls.

Electron Microscopy: Small blocks of tumor tissues were fixed in 2.5% buffered glutaraldehyde for 2 hr and postfixed with 1% buffered osmium tetroxide in 0.2 M cacodylate buffer for 1 hr. The blocks were embedded in epoxy resin and sectioned. Thin sections were stained with uranyl acetate and lead citrate, and examined in a JEM-100B electron microscope at 80 kV.

RESULTS

Original Tumor: The original tumor arose from subcutaneous tissue of the head of a 15-month-old male F344 rat, which was under the observation of a life-span study. When discovered, the tumor was a solid nodule, one cm in diameter. During the subsequent 2 months, it grew to a size of 4 cm in diameter accompanying by a bloody surface. The animal lost body-weight from 494 g to 443 g and became depressed. Therefore, the animal was subjected to a complete necropsy at the age of 17 months. The tumor was a nonencapsulated, firm mass weighing 25 g, and partially invaded the surrounding tissues, but no metastases were found. The cut surface of the tumor was white in color and was multilobular with a fascicular structure (Fig. 1). Microscopically, the tumor was high cellularity and contained irregularly defined areas of necrosis and hemorrhage. Densely populated areas were composed of a mixture of fibroblastic and histiocytic cells arranged in a storiform or cartwheel pattern (Fig. 2). Histiocytic cells had the abundant, eosinophilic cytoplasm and their nuclei appeared

dark and oval or round in shape. All cells were surrounded by reticulin fibers demonstrable by the Watanabe's silver impregnation. A moderate amount of collagenic fibers was present throughout tumor tissue. Sparsely populated areas were composed of cells containing Sudan Ⅲ- and oil red O-positive lipid droplets, and diastase-resistant PAS-positive material in their cytoplasm as well as fibroblastic and histiocytic cells. Bizarre giant cells were rarely found. Mitotic figures were frequent. Judging from these findings, the original tumor was diagnosed as the storiform type of MFH.

Serial Transplantation of MFH-MT in Syngeneic Rats:
In the 1st and 2nd passages, one half of the recipients developed MFH, whereas transplantability reached 100% positive from the 3rd passage onwards. There were no noticeable differences between tumor growths in different passage levels, except the 1st passage in which the tumor grew into a nodule of 2 cm in diameter 12 weeks after transplantation. The growth curve of tumors determined in the 9th generation is shown in Text-Fig. 1. A piece of tumor tissue developed into a nodule of 6 cm in

diameter, weighing 101 g on the average, 6 weeks after transplantation (Fig. 3). Recipients bearing large tumors died 8 to 9 weeks after transplantation, showing depression and emaciation. The weights of tumors removed from dead animals ranged from 244 to 320 g, and tumor:body-weight ratio was 65% on the average. Some nodules which evolved during the serial passages had cysts varying in size, containing transparent, sticky fluid. No metastatic lesions were found. The serially transplanted tumors were histologically indistinguishable from the original tumor.

Two predominant cell types, fibroblast-like cells and histiocyte-like cells, were also observed by electron microscopy. The former was characterized by the spindle-shaped, elongated cytoplasm, rich in dilated rough-surfaced endoplasmic reticulum and an elongated nucleus with prominent nucleoli. This type of cells was distributed in close association with bundles of collagenic fibers (Fig. 4). The latter had the abundant cytoplasm with many surface folds and indented or horseshoe-shaped nuclei. The cytoplasm contained lysosomes, well-developed Golgi apparatus, and rough-surfaced endoplasmic reticulum

(Fig. 5).

Neoplastic cells gave faintly to moderately positive reactions for ACP (Fig. 6), NSE, alpha-1 antitrypsin (Fig. 7) and lysozyme, and strongly positive reaction for ALP (Fig. 8). Positive reactions for S-100 protein, myoglobin, desmin, keratin, and factor Ⅷ-related antigen were not demonstrable in proliferating tumor cells, although the endothelial cells and peripheral nerves included in tumor tissues were positive for factor Ⅷ-related antigen and S-100 protein, respectively.

Histologic Diversity of MFH-MT Transplanted in Different Sites: Lung tumors, which developed 12 months after intravenous inoculation, and cutaneous tumors, which developed at the root of the tail 8 months after intradermal inoculation, were composed of a mixture of the pleomorphic, myxoid, giant cell, and storiform types. The pleomorphic type consisted of pleomorphic round cells and occasional giant cells. The myxoid type was composed of loosely arranged round, polygonal cells, and giant cells (Fig. 9), with intercellular material strongly positive for

alcian blue. Cells constituting the giant cell type had a large, lobulated nucleus with dense chromatin (Fig. 10). Osteosarcoma-like structures consisting of osteoblasts, osteoids, and calcifying areas were found in parts of the cutaneous tumor developed in the tail (Fig. 11). In the lung tumors, there were areas composed of elongated cells arranged in an interlocking pattern (Fig. 12) or round cells arranged in a compact sheet, and sclerosing hemangioma-like structures (Fig. 13). Occasional elongated cells gave a positive reaction for S-100 protein (Fig. 14).

Tumors, which developed in the subcutaneous tissue of the head and back 3 months after subcutaneous inoculation, and tumors, which developed in the parietal peritoneum and mesentery 3 months after intraperitoneal inoculation, possessed histologic characteristics of the storiform type similar to those of the original tumor.

Transplantation of MFH-MT into Athymic Nude Mice: Tumor grew in all nude mice of the 3 strains after subcutaneous transplantation with tumor tissues. No significant differences were observed in tumor

growth between both sexes and between the strains examined (Text-Fig. 2). At the end of the observation period of 5 weeks, tumors developed into nodules ranging in diameter from 1 to 3 cm, and in weight from 1 to 3 g (Fig. 15). All the tumors were well-circumscribed and had a watery appearance (Fig. 16), and there was neither infiltrative growth nor metastasis. They were composed mostly of pleomorphic cells, and gave a strongly positive reaction for alpha-1 antitrypsin (Fig. 17). The tumors were classified as the pleomorphic type of MFH.

Effects of Antitumor Drugs on MFH-MT: As shown in Text-Fig. 3, both CDDP and ADR caused a significant retardation of tumor development from 2 weeks after transplantation ($P < 0.05$, determined by the student's t test). The inhibitory effect appeared to be greater in the CDDP-treated group than in the ADR-treated group. At the end of the observation period of 5 weeks, tumor weights in the control, CDDP, and ADR groups were 31.2, 1.2, and 7.0 g, respectively. Tumors in rats which were treated with the antitumor drugs were composed predominantly

of fibroblast-like cells and plenty of collagenic fibers (Fig. 18). On the other hand, histiocyte-like cells appeared to decrease in number.

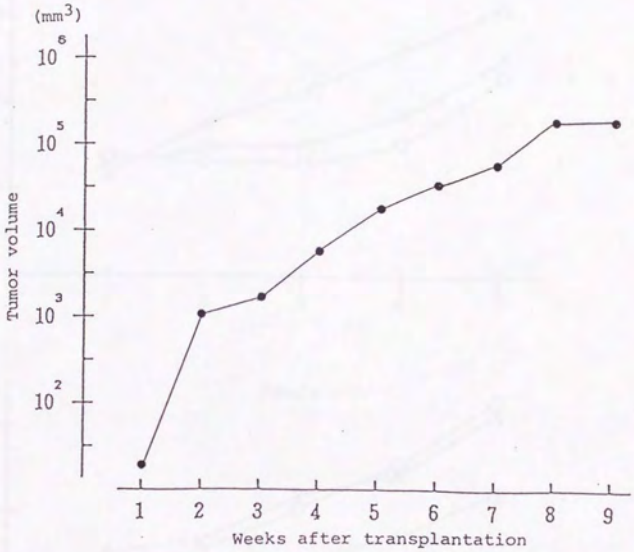

Text-Fig. 1. Growth curve of a transplantable malignant fibrous histiocytoma (MFH-MT) in F344 rats.

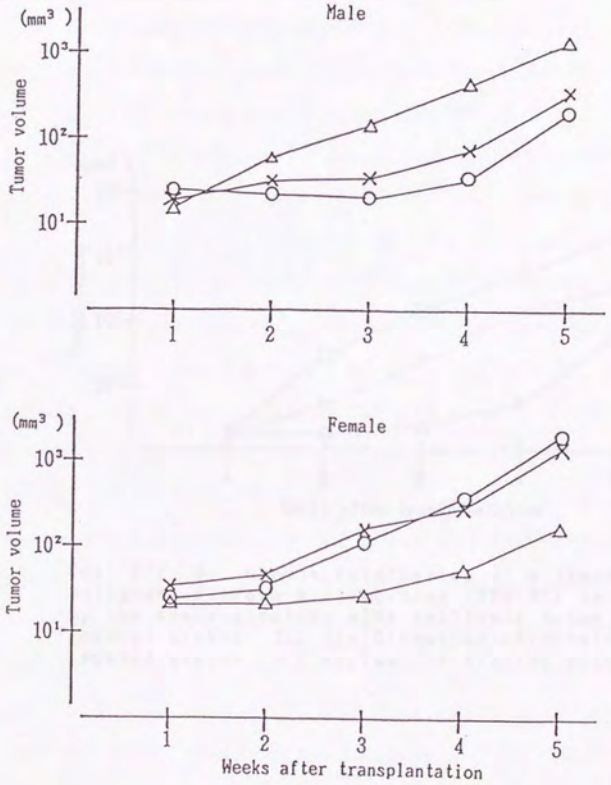

Text-Fig. 2. Growth curves of a transplantable malignant fibrous histiocytoma (MFH-MT) in athymic nude mice of three strains. (○, CRJ:CD-1(ICR)-nu/nu; ×, BALB/c-nu/nu slc; △, BALB/cA-Jcl-nu/nu).

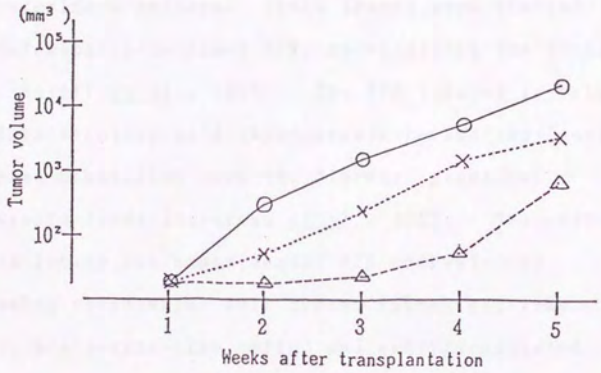

Text-Fig. 3. Growth retardation of a transplantable malignant fibrous histiocytoma (MFH-MT) in F344 rats by the administration with antitumor drugs. (○, control group; △, cis-Diamminedichloroplatinum-treated group; ×, adriamycin-treated group).

DISCUSSION

The original rat MFH and its serially transplanted tumors in syngeneic rats described here were composed mainly of fibroblastic and histiocytic cells arranged in a storiform pattern. These tumors were similar morphologically to human MFH, particularly the storiform type (Enjoji et al., 1980). The MFH induced in rats by administration of 4-(hydroxyamino)quinoline 1-oxide has been classified into the fibrous, giant cell, and myxoid types (Maruyama et al., 1983). The cell population in the experimental MFH consisted of following three major cell types: fibroblast-like cells, histiocyte-like cells, and undifferentiated cells possibly representing primitive mesenchymal cells (Maruyama et al., 1983). The predominant cell types in MFH-MT were fibroblastic and histiocytic cells, whereas no undifferentiated cells could be identified by both light and electron microscopy. Iwasaki et al. (1987) have thrown a doubt on the presence of undifferentiated cells in MFH, because these cells were indistinguishable from immature lymphoid cells scattering in the tumors. In MFH-MT, lipid-laden cells (xanthomatous cells) were often

seen in areas containing sparsely populated neoplastic cells as observed in human MFH, whereas giant cells were not so common as in human MFH (Enjoji et al., 1980). It has been suggested that xanthoma cells, giant cells, and cells possessing diastase-resistant PAS-positive material in their cytoplasm may originate from histiocytic cells (Maruyama et al.,1983; Nakanishi and Hizawa, 1984).

In enzyme/immunohistochemical examinations of MFH-MT, neoplastic cells gave faintly to moderately positive reactions for ACP, NSE, alpha-1 antitrypsin, and lysozyme, suggesting that the neoplastic cells may be of histiocytic origin. Positive reactivities to these stainings have frequently been demonstrated in human MFH, although the degree of reactions varied from case to case; the storiform type was shown to have a weaker reactivity than did the other types (Inoue et al., 1984; Nakanishi and Hizawa, 1984; Roholl et al., 1985a). Among these enzymes, alpha-1 antitrypsin has been reported to be the most reliable and useful marker for neoplastic cells forming MFH (Du Boulay, 1985; Roholl et al., 1985a). A strongly positive reaction for ALP was observed in cells of MFH-MT. Neoplastic cells constituting osteosarcomas

(Yoshida et al., 1988) and MFH (Roholl et al., 1986) were positive for ALP. Since osteosarcoma-like lesions have occasionally been found in experimentally induced rat MFH (Greaves et al., 1985) as seen in MFH-MT developed at the tail-root, cells with osteogenic potential may be comprised in MFH.

It has generally been accepted that MFH has a great histologic variability (Enjoji et al., 1980; Stiller and Katenkamp, 1981). Particularly, MFH-MT transplanted in the lungs and tail revealed a variety of histologic features. There were the storiform, pleomorphic, giant cell, and myxoid types as well as sclerosing hemangioma- and osteosarcoma-like structures. Areas consisting of elongated cells positive for S-100 protein were also observed. These findings seemed to support the hypothesis that MFH may originate from pluripotential mesenchymal stem cells (Brooks, 1986).

MFH-MT grew well in athymic nude mice of three strains. The tumors developed in these mice appeared to consist mostly of pleomorphic cells, which showed more strongly positive reaction for alpha-1 antitrypsin than did MFH-MT with a storiform pattern, suggesting a possible modification of

property in neoplastic cells. Similar results have been obtained by Shirasuna et al. (1985) in nude mice inoculated with cloned cells established from human MFH. On the other hand, xenografts in nude mice of two cell lines derived from human MFH retained histologic features of the original tumor (Roholl et al., 1986).

ADR and CDDP have been demonstrated to have a broad range of antitumor activity against human and animal tumors (Di Marco et al., 1969; Kociba et al., 1970). The development of MFH-MT was significantly retarded by both ADR and CDDP. It is interesting to note that MFH-MT, which had been treated with the drugs, was composed almost entirely of fibroblast-like cells and abundant collagenic fibers, whereas histiocyte-like cells were markedly decreased in number. These observations produce further evidence to show that MFH is heterogeneous and composed of cell types with different susceptibilities to antitumor drugs.

SUMMARY

Spontaneously occurring MFH was found in subcutaneous tissue of the head of a 15-month-old male F344 rat. The tumor was serially transplanted into syngeneic rats up to the 45th generation, and the transplantable tumor was designated MFH-MT. Light and electron microscopic observations revealed that the original MFH and MFH-MT were composed of an admixture of fibroblastic and histiocytic cells arranged in a storiform pattern. Neoplastic cells gave positive reactions for acid phosphatase, alkaline phosphatase, nonspecific esterase, alpha-1 antitrypsin, and lysozyme. The tumors transplanted into the lungs and cutaneous tissue of the tail had a mixed histologic appearance of the storiform, pleomorphic, myxoid, and giant cell types. Moreover, sclerosing hemangioma- and osteosarcoma-like structures were also found. MFH-MT grew well in athymic nude mice showing neoplastic proliferation of pleomorphic cells strongly positive for alpha-1 antitrypsin. The development of MFH-MT was significantly retarded by the two antitumor drugs tested. The retarded tumors consisted predominantly of fibroblastic cells and abundant collagenic fibers.

CHAPTER 2

CHARACTERISTICS OF *IN VITRO* PASSAGED CELLS DERIVED FROM A TRANSPLANTABLE RAT MALIGNANT FIBROUS HISTIOCYTOMA (MFH-MT)

INTRODUCTION

Cell lines established from human malignant fibrous histiocytoma (MFH) by Iwasaki et al. (1982) and Shirasuna et al. (1985) had fine structural characteristics of histiocytes and showed histiocytic functional markers. On the contrary, Roholl et al. (1986) cultivated two cell lines each from a human MFH. The culture of the first tumor consisted of cells resembling primitive mesenchymal cells and that of the second tumor showed features of fibroblastic cells. These observations suggest that a group of human MFH is heterogeneous.

There have been no reports dealing with cultured cells from spontaneous rat MFH. In Chapter 1, the author described that a transplantable rat MFH (MFH-MT) showed various histologic appearances, in agreement with cases of human MFH. In an attempt to clarify the histogenesis of MFH-MT, characteristics of in vitro passaged cells (MT-P) derived from MFH-MT were pursued morphologically and functionally, and tumors induced in syngeneic rats by inoculating MT-P were histologically investigated. This chapter describes results obtained in these studies.

MATERIALS AND METHODS

Tissue Culture: Tumor tissues removed aseptically from MFH-MT at passage 24 were minced with scissors and dispersed with 0.2% trypsin in phosphate-buffered saline (PBS). The cells were washed twice in PBS and grown in culture flasks. The growth medium used was Dulbecco's minimum essential medium (MEM) (GIBCO, Grand Island, NY) supplemented with 10% fetal bovine serum (GIBCO), streptomycin (100 μg/ml) and penicillin (100 U/ml). The cultures were incubated at 37℃ in a closed atmosphere or a humidified, 5% CO_2 atmosphere. Confluent cell sheets were treated with a mixture of 0.1% trypsin and 0.02% ethylene-diaminetetraacetic acid in PBS, and cells were subcultured at 7- to 12-day intervals. MT-P used in the following experiments were at passages 9 to 24.

Observations of MT-P: For light microscopic observations, MT-P grown on tissue culture chamber slides (LAB-TEK, Miles, IL) were fixed in Bouin's fluid or 4% formol calcium at 4 ℃ for 1-2 hr. The fixed MT-P were stained with hematoxylin and

eosin (HE), periodic acid-Schiff (PAS) with and without diastase digestion, and oil-red O. They were also stained by the Gomori's method for acid phosphatase (ACP)(pH 5.0), by the alpha-naphthyl acetate method for nonspecific esterase (NSE)(pH 7.4), and by the naphthol AS method for alkaline phosphatase (ALP)(pH 9.0). For electron microscopy, cell pellets formed by centrifugation were fixed and embedded by the conventional method as described in Chapter 1. Sections were stained with uranyl acetate and lead citrate and examined in a JEM-100B electron microscope at 80 kV.

Assays for Immunorosette Formations: Rosette formation assays for Fc- and C3-receptors were carried out as described by previous workers (Iwasaki et al., 1982; Tanaka, H. et al., 1982; Yumoto and Morimoto, 1980).

Anti-sheep red blood cell (SRBC) serum for the Fc-receptor assay was prepared by inoculating 20-week-old male F344 rats intraperitoneally with 2 ml of a 20% SRBC suspension in PBS. The rats were bled after inoculating 7 times in the course of 4 weeks. Anti-SRBC serum for the C3-receptor assay was obtained from 20-week-old male F344 rats

3 days after intravenous inoculation with 2 ml of a 20% SRBC suspension in PBS. Both sera were inactivated by heating at 60℃ for 30 min. Normal serum collected from 20-week-old male F344 rats was used as complement for the C3-receptor assay. SRBCs incubated with antiserum for the Fc-receptor assay or SRBCs incubated with both antiserum and normal serum for the C3-receptor assay were mixed with 5×10^7 test cells suspending in MEM. After being incubated at 37℃ for 20 to 30 min, the cells were stained with brilliant cresyl blue. Positive rosettes were expressed as percentage of test cells with three or more adhering SRBCs to 400 test cells.

Assays for Phagocytic Activity: After being washed in MEM, cells grown on chamber slides for 24 hr were incubated with 0.3 ml of MEM containing 0.1% latex particles (0.78 μm : Cosmo Bio. Co., Ltd.) or with 0.3 ml of 0.5% SRBC incubated with antiserum for the Fc-receptor assay in MEM for 60 and 120 min at 37℃. Slide preparations were fixed in methanol and stained with May-Grünward Giemsa or HE. Positive cells for phagocytosis were expressed as percentage

of phagocytes to 400 cells examined with the microscope.

Chromosomal Analysis: Confluent cell sheets were exposed to colchicine in a concentration of 0.5 μg/ml for 3 hr. After being suspended in a hypotonic solution, cells were fixed in a mixture of methanol 3 : acetic acid 1 and stained with Giemsa. Chromosomes in 100 cells were counted.

Observations of Tumors Developed in Syngeneic Rats Inoculated with MT-P: One ml of 10^7 cells/ml PBS was inoculated subcutaneously or intraperitoneally into syngeneic rats, 10-25 weeks of age. The animals (F344/DuCrj rats) used were produced in the author's laboratory and maintained in a barrier room. Tumors removed from all the animals were weighed and fixed in 10% neutral buffered formalin. They were embedded in paraffin, sectioned, and stained with HE, PAS with and without diastase digestion, Watanabe's silver impregnation for reticulin, azan-Mallory and alcian blue (pH 2.5). Paraffin-embedded sections from tumors were also stained by the peroxidase-antiperoxidase technique using a commercial kit (Universal Immuno-peroxidase Staining Kit, Cambridge Research Laboratory

(CRL), MA). Rabbit antisera to alpha-1 antitrypsin (CRL), S-100 protein (CRL), factor Ⅷ-related antigen (CRL), and myoglobin (CRL) were used as primary antibodies. Frozen sections from fresh specimens were also examined enzymehistochemically for ACP, NSE, and ALP by the methods described in Chapter 1.

RESULTS

Characteristics of MT-P: Cells grown in glass culture flasks had variable morphologic features, such as spindle, polygonal, and giant cell types (Fig. 19). The polygonal cells were most predominant in MT-P, and they had the abundant cytoplasm and a large, round nucleus with some nucleoli. The spindle cells were elongated in shape and had an oval nucleus. The giant cells occasionally developed in areas of less cellularity and they had large, pale and often multilobulated nuclei with several prominent nucleoli. In densely populated areas, these cells became somewhat elongated and were arranged in a storiform pattern or formed foci. PAS-positive material digestible with diastase was often found in their cytoplasm. The cytoplasm of occasional cells contained globular fat droplets demonstrable with oil red O staining.

Ultrastructurally, the polygonal and giant cells had indented nuclei with large distinct nucleoli and many cytoplasmic extensions. In their cytoplasm, there were many lysosomes, slightly dilated rough-surfaced endoplasmic reticulum, moderate number of mitochondria, and phagosomes containing cellular

debris (Fig. 20). Glycogen granules apparently corresponding to PAS-positive material seen by light microscopy were also present in the cytoplasm. The spindle cells had the smooth cell surface, an elongated nucleus, and the cytoplasm with a small number of lysosomes.

MT-P were moderately positive for ACP (Fig. 21) and NSE (Fig. 22), expressing coarse perinuclear cytoplasmic granules, and strongly positive for ALP.

Immunorosette Formation and Phagocytic Activity:
The rosette formation by Fc-receptors was demonstrated in 20% of MT-P with anti-SRBC serum, whereas that by C3-receptors was found in 11% of the cells. SRBCs, which were incubated with antiserum for the Fc-receptor assay, were phagocytized by 17% and 18% of MT-P after incubation at 37℃ for 60 and 120 min, respectively. Latex particles treated by the same way were phagocytized by 10% and 12% of the cells after the same periods of incubation (Fig. 23).

Chromosomal Analysis: Chromosomal analysis was carried out in cultured cells from passage 10. Chromosome numbers ranged widely from 32 to 100

with two peaks of 64 and 76 as shown in Text-Fig. 1.

Characteristics of Tumors Induced in the Rats by Inoculating MT-P: All the rats, which were inoculated subcutaneously or intraperitoneally with MT-P, developed tumors. When inoculated intraperitoneally, a large number of nodules 0.5-1.5 cm in diameter developed on the parietal peritoneum and mesentery of the rats 5 weeks after inoculation. Neither infiltrative growth to the visceral organs nor ascites was observed. In animals inoculated subcutaneously, tumors became palpable 2 weeks after inoculation. The tumors removed from recipients ranged in weight from 157 to 245 g and in diameter from 4 to 5 cm eight to nine weeks after inoculation. They were well-circumscribed and firm masses with multilobular structure. The cut surface of the tumors was white in color and had irregularly defined central areas of necrosis and hemorrhage. Grayish ossifying tissues were sporadically detected in subcutaneous tumors.

Microscopically, all the tumors had variable histologic patterns. They were composed partly of histiocytic cells arranged in a compact sheet (Fig. 24).

The cells were round, ovoid or often fusiform in shape and had the abundant eosinophilic cytoplasm with an oval nucleus. Aggregations of histiocytic cells containing PAS-positive, diastase-digestible material in their cytoplasm were frequently seen (Fig. 25). Fibroblastic spindle cells often formed a storiform pattern (Fig. 26), and loosely arranged polygonal and elongated cells were supported by intercellular material positive for alcian blue (Fig. 27). All tumor cells were surrounded by reticulin fibers demonstrable by the Watanabe's silver impregnation. In sections stained by the azan-Mallory method, collagenic fibers were scanty in tumor tissues, except areas with a storiform pattern. Bizarre giant cells and mitotic figures were frequently found. Ossifying tissues were composed of osteoblasts, osteoid tissue, and calcifying areas, giving an appearance of osteosarcoma (Fig. 28).

Neoplastic cells gave moderately positive reactions for ACP, NSE (Fig. 29), ALP (Fig. 30), and alpha-1 antitrypsin. Occasional cells were positive for S-100 protein. Myoglobin and factor Ⅷ-related antigen were negative in tumor cells.

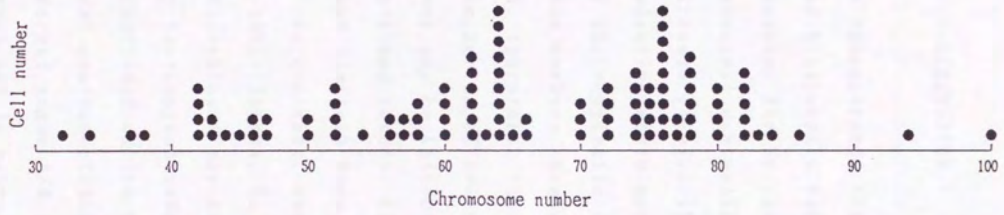

Text-Fig. 1. Distribution of chromosome numbers in 100 cells of MT-P.

DISCUSSION

It has been demonstrated that cells cultivated from human MFH had histiocytic markers such as immunorosette formation for Fc- and C3-receptors, phagocytic and lysosomal enzymatic activities (Iwasaki et al., 1982; Shirasuna et al., 1985). In MFH induced in mice by transplanting mouse peritoneal macrophages transformed by SV 40, neoplastic cells also expressed similar histiocytic markers (Hagari and Yumoto, 1987). It was considered, therefore, that MFH may be derived from a histiocytic series of cells, and that fibroblastic cells in the tumors may be interpreted as facultative fibroblasts (Hagari and Yumoto, 1987; Iwasaki et al., 1982; Strauchen and Dimitriu-Bona, 1986; Yumoto and Morimoto, 1980). In contrast, some investigators (Krawisz et al., 1981; Tanaka, H. et al., 1982) have considered that fibroblasts may have the capacity to transform into histiocytes under certain conditions. It was recently concluded on the basis of phenotypic and ultrastructural characteristics of cell lines derived from different human MFH that a group of MFH is heterogeneous and is probably derived from more than one progenitor cell (Roholl et al., 1986).

In the present study, MT-P exhibited both immunorosette formation and phagocytic activity at frequencies of 10-20% and showed moderately positive reactions to lysosomal enzymatic activities of ACP and NSE. Ultrastructurally, many lysosomes were observed in the cytoplasm of polygonal and giant cells. Moreover, tumors developed in the rats after inoculating MT-P contained neoplastic cells positive for ACP, NSE, and alpha-1 antitrypsin. These enzymatic activities have frequently been demonstrated in human MFH and regarded as reliable markers for MFH (Inoue et al., 1984; Nakanishi and Hizawa 1984; Roholl et al., 1985ab). Our results produce evidence indicating that cells with histiocytic markers are comprised in MFH-MT.

Human MFH has variable histologic patterns (Enjoji et al., 1980; Stiller and Katenkamp, 1981), and has been classified into the storiform, pleomorphic, myxoid, xanthogranulomatous, and giant cell types (Enjoji et al., 1980). Tumors induced in the rats by inoculating MT-P had variable morphologic patterns, such as the pleomorphic, storiform, and myxoid types. This suggests that heterogeneous cell types may be comprised in MFH-MT. The cells with glycogen granules,

as demonstrated by the PAS method and electron microscopy, were frequently seen in the induced tumors, while such cells were rarely seen in the original tumors and serially passaged MFH-MT. These observations suggest that serial passages in cell culture may have brought on a change in predominant cell types.

Osteosarcoma-like structure was sporadically observed in subcutaneous tumors induced in the rats and neoplastic cells gave a positive reaction for ALP. Neoplastic cells constituting human osteosarcoma have been reported to be positive for ALP (Yoshida et al., 1988). Accordingly, MT-P may contain a precursor cell capable of differentiating into osteogenic cells.

SUMMARY

Morphologic and functional characteristics on *in vitro* passaged cells (MT-P) derived from a transplantable rat malignant fibrous histiocytoma (MFH-MT) were pursued. There were the spindle, polygonal, and giant cell types in MT-P. Ultrastructurally, the polygonal and giant cells had the abundant cytoplasm with many lysosomes and processes, whereas the spindle cells possessed the smooth cell surface and a small number of lysosomes in their cytoplasm. Immunorosette formation for Fc- and C3-surface receptors and phagocytic activity were demonstrated in 10-20% of MT-P. MT-P were positive for acid phosphatase, nonspecific esterase, and alkaline phosphatase. Chromosomes counted in 100 MT-P ranged from 32 to 100 with two peaks of 64 and 76. Tumors induced in syngeneic rats by inoculating MT-P showed variable histologic patterns. They were composed partly of histiocytic cells arranged in a compact sheet. Fibroblastic cells were often arranged in a storiform pattern or were supported by myxoid matrix. Osteosarcoma-like structures were

occasionally found in the tumors. These results suggest that MFH-MT is heterogeneous, although some cells constituting the tumors have histiocytic markers.

CHAPTER 3

GLYCOSAMINOGLYCANS IN A TRANSPLANTABLE RAT MALIGNANT FIBROUS HISTIOCYTOMA (MFH-MT)

INTRODUCTION

Malignant fibrous histiocytoma (MFH) in humans has highly variable histologic patterns and has been classified into the storiform, pleomorphic, myxoid, xanthogranulomatous, and giant cell types. The myxoid type was defined as an MFH in which more than one-half of its cut surface has a myxoid appearance (Enjoji et al., 1980; Stiller and Katenkamp, 1981). Myxoid areas were often observed in a transplantable rat MFH (MFH-MT) established by the author and in tumors induced in syngeneic rats by inoculating in vitro passaged cells (MT-P) derived from MFH-MT. The histologic features of these tumors have been described in detail in Chapters 1 and 2. The myxoid areas were composed of sparsely populated spindle cells and polygonal cells supported by intercellular material stained positively with alcian blue and negatively by the periodic acid-Schiff reaction. It has been suggested that a stroma of myxoid areas contains glycosaminoglycans (GAG) (Hagari and Yumoto, 1987). GAG consist of hyaluronic acid (HA), chondroitin sulfate A (ChS-A), chondroitin sulfate B (dermatan sulfate, DS), chondroitin sulfate C (ChS-C), keratan

sulfate (KS) and heparin (HeP). In this Chapter, GAG in MFH-MT were identified by the histochemical stainings and cellulose acetate electrophoresis (CAE).

MATERIALS AND METHODS

Histochemical Stainings: Tumors examined histochemically were as follows: MFH-MT at passage 26 (MT-26) which had been serially passaged in syngeneic rats by subcutaneous transplantation; tumors induced in the tail-root of syngeneic rats by intradermal transplantation of MFH-MT (MT-RT); tumors induced in subcutaneous tissue of CRJ:CD-1 (ICR)-nu/nu nude mice by subcutaneous transplantation of MFH-MT (MT-NU); and tumors induced in syngeneic rats by intraperitoneal inoculation with MT-P (MT-PT). Sections prepared from all these tumors contained myxoid areas as described in Chapters 1 and 2. Enzymes used in histochemical examinations were bovine testicular hyaluronidase (BH) (Sigma Chemical Co., St. Louis), streptomyces hyaluronidase (SH) (Seikagaku Kogyo Co., Ltd), chondroitinase ABC (C-ABC) (Sigma), and chondroitinase AC (C-AC) (Sigma). Specificity of these enzymes for GAG degradation was as follows: BH for HA, DS, ChS-A, and ChS-C; SH for HA; C-ABC for HA, DS, ChS-A, and ChS-C; C-AC for ChS-A and ChS-C (Chiarugi et al., 1978).

BH was dissolved at 100 turbidity reducing units (TRU)/ml in 0.2 M acetate buffer, pH 5.6.

Sections were incubated with the BH solution at 37℃ for 3 hr. SH was dissolved at 50 TRU/ml in 0.1 M phosphate buffer, pH 6.0. Sections were incubated with the SH solution at 60℃ for 4 hr. C-ABC and C-AC were dissolved in a concentration of 1-2 unit/ml in 0.1 M tris-HCl buffer, pH 8.1 and pH 7.4, respectively. Sections were incubated with the C-ABC solution or C-AC solution at 37℃ for 2 hr. After being incubated with the enzymes, sections were stained with alcian blue (pH 2.5) and nuclear fast red. Control sections were processed in each of the buffers without the enzymes under the same conditions and stained.

CAE: Two samples of sticky cyst-fluid (C42-2 and C42-3) which were collected from MFH-MT at passage 42 in syngeneic rats, and culture medium which was collected 5 and 13 days after seeding passage 24 of MT-P (TC-5 and TC-13) were analyzed by CAE as will be described below. Culture medium incubated for 5 days in the absence of MT-P was analyzed in a like manner and served as the negative control (TC-C). Medium used for cell culture was Dulbecco's minimum essential medium (GIBCO, Grand Island, NY)

supplemented with 10% fetal bovine serum (GIBCO), streptomycin (100 μg/ml) and penicillin (100 U/ml). Characteristics of MT-P have been described in Chapter 2.

Extraction of GAG and electrophoresis were performed according to the methods described by Hagari and Yumoto (1987). Briefly, 4-5 ml of the samples was diluted with an equal volume of distilled water and centrifuged at 3,000 rpm for 5 min. Six ml of the supernatant was treated with acetone for 30 min and then with ether for 30 min twice. The precipitate was treated with 0.5 M NaOH for 20 hr at 4℃ and neutralized with 1 N HCl. The solution was boiled for 30 min and then digested with protease (Sigma) for 24 hr at 50℃. Trichloroacetic acid (30% w/v) was added to the final concentration of 10%. After being kept for 1 hr at 4℃, the mixture was centrifuged at 8,000 x g for 15 min at 0℃. The supernatant was dialyzed in a cellulose tube against distilled water for 48 hr. Thereafter the samples were powdered by freeze-drying for 24 hr.

The extracted samples and standard GAG including HA, DS, ChS-A, ChS-C, HeP, and KS (Sigma) were dissolved in distilled water at concentrations of 0.5-1 mg/ml.

For electrophoresis 2 μl of these solutions was applied at 1 cm from the negative electrode on a 6 x 8 cm cellulose acetate sheet which had been presoaked in 0.1 M pyridine-formic acid buffer, pH 3.0. The sheets were subjected to electrophoresis for 10 min at 180 V in the same buffer and subsequently stained with alcian blue (pH 2.5). The samples of C42-3, TC-13, standard HA, and standard ChS-A were incubated twice in an SH solution (25 TRU/ml) for 24 hr at 50℃ and these samples were then subjected to CAE.

RESULTS

MT-26, MT-RT, MT-NU, and MT-PT were similar histologically to each other in results of alcian blue stain combined with enzymatic degradation. GAG in tumor tissues were completely digested by BH, moderately by C-ABC and C-AC, and faintly by SH, compared with controls positive to the alcian blue stain (Figs. 31 and 32). These results demonstrated that the intercellular matrix of myxoid areas contained both HA and ChS.

In CAE, the bands of C42-2, C42-3, TC-5, and TC-13 appeared to correspond to those of the standard HA, but did not correspond to those of the other standard GAG such as DS, ChS-A, ChS-C, HeP, and KS (Figs. 33 and 34). The band of TC-C did not appear on the sheet (Fig. 34). C42-3, TC-13, and standard HA were degraded when treated with SH solution which digests only HA (Fig. 35). However, part of the band of C42-3 which slightly migrated toward the positive electrode was not degraded, probably due to the difference in molecular size. The results of CAE suggested that cells constituting MFH-MT may secrete HA.

DISCUSSION

The presence of HA has histologically been demonstrated in human MFH (Roholl et al., 1986) and in mouse MFH induced by intraperitoneal inoculation of peritoneal macrophages transformed by SV 40 (Hagari and Yumoto, 1987). In these mice HA was also identified in their ascites by CAE (Hagari and Yumoto, 1987). There have been no reports on GAG in rat MFH.

HA, which was synthesized at the inner side of the plasma membranes (Prehm, 1984), has been known to play an important role in the development of embryonal and primitive cells (Le Douarin, 1984; Singley and Solursh, 1981). HA has also been shown to be present in a variety of neoplastic tissues (Chiarugi et al., 1978; Chiu et al., 1984). Particularly, mesothelioma has been reported to secrete a considerable amount of HA, that was regarded as one of the diagnostic criteria for this tumor (Chiu et al., 1984; Wagner et al., 1962). Experimentally induced mesotheliomas in rats were considered to be derived from a multipotential cell capable of differentiating into both fibroblasts and epithelial cells (Brown et al., 1985). In this study,

it was confirmed that HA was produced by neoplastic cells constituting MFH-MT, suggesting that neoplastic cells of MFH-MT might be at an embryonal and undifferentiated stage, as mentioned by Roholl et al. (1986). Mammary tumors with cartilaginous tissue and osteoids of dogs contained both HA and ChS in their extracellular matrix (Palmer and Monlux, 1979). Both HA and ChS demonstrated in MFH-MT by the present histochemical examinations may be related to osteogenesis, since an osteosarcoma-like structure consisting of osteoblasts, osteoids, and calcifying tissue was sporadically found in MFH-MT as described in the first and second chapters.

Recently, GAG have been studied in association with tumor malignancy such as invasiveness, adhesiveness, and metastasis (Angello et al., 1982; Becker et al., 1986; Chiarugi et al., 1978; Vannucchi and Chiarugi, 1976). Exogenous cell growth factor has been shown to exist in GAG produced by bone marrow stromal cells (Gordon et al., 1987). These observations may explain the relationship between cell growth and GAG.

SUMMARY

Glycosaminoglycans (GAG) in a transplantable rat malignant fibrous histiocytoma (MFH-MT) were identified by the histochemical stainings and cellulose acetate electrophoresis (CAE). GAG in tumor tissues of MFH-MT were completely digested by bovine testicular hyaluronidase, moderately by chondroitinase ABC and chondroitinase AC, and faintly by streptomyces hyaluronidase, compared with controls positive to the alcian blue stain. These results demonstrated that the intercellular matrix of myxoid areas in MFH-MT contained both hyaluronic acid (HA) and chondroitin sulfate. In CAE, the bands of GAG, which had been isolated from cyst-fluid of MFH-MT and from culture medium of in vitro passaged cells (MT-P) derived from MFH-MT, corresponded to those of the standard HA. The results of CAE demonstrated that cells constituting MFH-MT secrete HA, suggesting that neoplastic cells of MFH-MT might be at an embryonal and undifferentiated stage.

CHAPTER 4

CHARACTERISTICS OF *CIS*-DIAMMINEDICHLOROPLATINUM-SELECTED *IN VITRO* PASSAGED CELLS DERIVED FROM A TRANSPLANTABLE RAT MALIGNANT FIBROUS HISTIOCYTOMA (MFH-MT)

INTRODUCTION

Malignant fibrous histiocytoma (MFH) consists predominantly of fibroblastic and histiocytic cells, and is often mixed with pleomorphic giant cells, xanthoma cells, and varying numbers of inflammatory cells (Enjoji *et al.*, 1980; Konishi *et al.*, 1982; Stiller and Katenkamp, 1981). The precise mechanism of the histogenesis of MFH has not been fully elucidated, despite extensive studies by many workers.

It was confirmed in Chapter 2 of this series of studies that *in vitro* passaged cells (MT-P) derived from a transplantable rat MFH (MFH-MT) comprised cells with histiocytic markers. However, tumors induced in syngeneic rats by inoculating MT-P showed histologic variability; osteosarcomatous lesions were sporadically observed in the tumors, suggesting cells with osteogenic potential might be present in MFH-MT. The sensitivity test of MFH-MT to antitumor drugs described in Chapter 1 revealed that there were cell types having different susceptibilities to the antitumor drugs. In the present work, the author selected a cell line (MT-R10) from MT-P by using an antitumor drug, *cis*-Diamminedichloroplatinum (CDDP). In order to obtain further information on the

histogenesis of MFH, characteristics of MT-R10 and tumors induced in rats by inoculating MT-R10 were investigated in comparison with those of MT-P. This chapter describes the results obtained in these studies.

MATERIALS AND METHODS

Derivation of CDDP-Selected Cells: The preparation of MT-P from MFH-MT has been described in Chapter 2. The growth medium used was Dulbecco's minimum essential medium (MEM) (GIBCO, Grand Island, NY) supplemented with 10% fetal bovine serum (GIBCO), streptomycin (100 μg/ml) and penicillin (100 U/ml). The antitumor agent used was CDDP obtained from Nippon Kayaku Co., Ltd. (Tokyo, Japan). The techniques used for the induction of CDDP-selected cells were based on those described previously (Kikuchi et al., 1986). MT-P were initially cultivated twice in MEM containing 0.05 μg CDDP/ml. Subsequently, cells capable of proliferating in the presence of 0.05 μg CDDP/ml were serially passaged in MEM with CDDP at increasing concentrations of 0.1, 0.2, 0.5, and 1.0 μg/ml. The cells in each concentration were passaged two or three times at 16- to 20-day intervals. MEM containing CDDP was changed every four days. The cells that were able to proliferate in the presence of the highest concentration (1.0 μg/ml) of CDDP were then passaged in CDDP-free MEM and designated MT-R10. The cells grown in the presence of 0.2 μg CDDP/ml (MT-R2) were also used for some experiments.

In vitro Observations of CDDP-Selected Cells:
Growth of MT-P and MT-R10 at passage 1 (MT-R10/1) and passage 10 (MT-R10/10) in CDDP-free MEM was observed. One ml of 10^4 cells/ml MEM was seeded in each well of a 24-well multidish (24 well/flat bottom, Corning Glass Works, Corning, NY), and the cultures were incubated in a humidified atmosphere of 5% CO_2 at 37℃. At 1, 2, 3, 5, 7, and 9 days after seeding, cells in each well were harvested and counted using a hemocytometer. Triplicate cultures were counted and the cell viability was assessed by trypan blue dye exclusion. The doubling time was determined from cell numbers counted 3 and 5 days after seeding.

The sensitivity to CDDP of MT-P, MT-R10/1, and MT-R10/10 was determined as follows (Kikuchi et al., 1986): 10^4 cells were seeded in each well of a 24-well multidish; at 2 days postseeding, various concentrations of CDDP were added to the medium. After additional 3 days of cultivation, viable cells in each well were counted in triplicate cultures. The mean percentages of viable cells at each concentration were calculated relative to viable cells grown in CDDP-free MEM for 5 days.

MT-R2 and MT-R10 were examined by light and electron microscopy using the methods as described for MT-P in Chapter 2.

Immunorosette formations for Fc- and C3-receptors and phagocytosis of latex particles were assayed in MT-R10 at passage 8 by the conventional methods as described in Chapter 2. Chromosomal analysis was performed in MT-R10 at passage 8, and chromosomes in 50 cells were counted as described in Chapter 2.

In vivo Observations of CDDP-Selected Cells:

One ml of 10^7 cells/ml phosphate-buffered saline of MT-R2, MT-R10/1 or MT-R10/10 was inoculated subcutaneously into syngeneic male F344 rats, 10-25 weeks old. The diameters of all the tumors that subsequently developed in subcutaneous tissue were measured once weekly with calipers. Tumor masses induced by inoculating MT-R10/10 were minced into small pieces, < 2 mm in diameter, with scissors, and then transplanted subcutaneously at the interscapular region of syngeneic rats through a trocar with a diameter of 2 mm. The tumors were serially transplanted every 5 to 6 weeks.

Tumors removed from all the animals were

weighed and fixed in 10% neutral buffered formalin. They were then embedded in paraffin, sectioned, and stained with hematoxylin and eosin (HE), periodic acid-Schiff (PAS) with and without diastase digestion, Watanabe's silver impregnation for reticulin, azan-Mallory and alcian blue (pH 2.5). Paraffin-embedded sections were also stained by the peroxidase-antiperoxidase technique using commercial kits (Universal Immunoperoxidase Staining Kit; Cambridge Research Laboratory (CRL), MA, or DAKO PAP Kit; DAKO Corp., Santa Barbara, CA). Rabbit antisera against alpha-1 antitrypsin (CRL), S-100 protein (CRL), lysozyme (CRL), keratin (CRL), factor Ⅷ-related antigen (DAKO), and desmin (DAKO) were used as primary antibodies. For the indirect immunoperoxidase method, paraffin-embedded sections were reacted with 100-fold-diluted anti-rat monocytes/ macrophages monoclonal antibody (MAB1435, Chemicon International Inc., CA) and 400-fold diluted peroxidase-conjugated affinipure goat anti-mouse IgG, Fc fragment antibody (Jackson Immunoresearch Laboratories, Inc., PA) as secondary antibodies. In these immunoperoxidase stainings, diaminobenzidine tetrahydrochloride or 3-amino-9-ethylcarbazole was used as a substrate, and the sections were counterstained with hematoxylin.

Frozen sections from fresh specimens were examined histochemically for acid phosphatase (ACP), nonspecific esterase (NSE), and alkaline phosphatase (ALP) by the methods as described in Chapter 1.

RESULTS

The growth curves of MT-P, MT-R10/1, and MT-R10/10 are shown in Text-Fig. 1. No significant difference was noted between the growth of MT-P and that of MT-R10/10. The doubling times of MT-P and MT-R10/10 were 25.5 and 22.3 hr, respectively. In contrast, the doubling time of MT-R10/1 was 233.1 hr, showing remarkably slower growth.

As shown in Text-Fig. 2, the cell proliferation of MT-P, MT-R10/1, and MT-R10/10 was dose-dependently suppressed at all the concentrations of CDDP examined. The CDDP concentrations required for 50% suppression of MT-P, MT-R10/10, and MT-R10/1 proliferation were 0.075, 0.15, and 1.15 μg/ml, respectively.

Rosette formations for Fc- and C3-receptors and phagocytosis of latex particles were observed in < 3% of MT-R10 cells. The chromosomal numbers in MT-R10 ranged from 46 to 105 with a peak of 88 (Table 1) (Text-Fig. 3).

MT-R10 cells had a round, abundant cytoplasm and an ovoid nucleus with one to several prominent nucleoli giving an epithelial appearance (Fig. 36). The cells were arranged in a compact sheet and

piled up forming foci when confluent. PAS-positive, diastase-digestible material was occasionally found in their cytoplasm. Morphologic modulation was not observed in serially passaged MT-R10. Ultrastructurally, MT-R10 cells appeared dark and had the slightly irregular cell surface and an ovoid nucleus with prominent nucleoli. Their cytoplasm contained numerous free ribosomes, some mitochondria with an electron-dense matrix, occasional aggregations of glycogen granules, and other poorly developed organelles (Fig. 37).

MT-R2 showed a moderate reaction for ACP and NSE, as did MT-P, whereas MT-R10 gave faintly positive or negative reactions for these enzymes. MT-R2 and MT-R10 were strongly reactive for ALP (Table 1).

All of MT-R2, MT-R10/1, and MT-R10/10 were tumorigenic when inoculated subcutaneously into rats. The induced tumors became palpable three to five weeks after inoculation. They grew into nodules ranging in diameter from 2 to 4 cm and weighing between 10 and 60 g six to seven weeks after becoming evident by palpation. There was no marked difference in tumor growth between the cell lines. Tumors induced by MT-R2 were hard, well-circumscribed and multilobulated

with a fascicular structure, whereas those induced by MT-R10/1 and MT-R10/10 were grayish and fragile without a multilobular or fascicular structure. All of these tumors often contained ossifying areas in their center.

Tumors induced by inoculation with MT-R2 were composed of fibroblastic and histiocytic cells arranged in a storiform pattern (Fig. 38). A moderate number of collagenic fibers staining blue by the azan-Mallory method were present among the neoplastic cells. Some areas of the tumors consisted of loosely arranged polygonal and round cells supported by myxoid material positive for alcian blue (Fig. 39). Neoplastic cells showed moderate reactions for NSE (Fig. 40) and ACP, and a strong reaction for ALP.

The tumors induced by inoculation with MT-R10/1 and MT-R10/10 closely resembled each other. They were composed predominantly of small, round, undifferentiated cells with the scanty cytoplasm and oval, hyperchromatic nuclei often arranged in a compact sheet (Fig. 41). They also showed organoid structures that were formed by neoplastic cells proliferating around vascular channels (Fig. 42) or trabecular structures consisting of thick cords of

neoplastic cells (Fig. 43). Mitotic figures and necrotic foci were often seen in these tumors. There were no demonstrable collagenic fibers in the tumor tissues. Tumor cells often contained PAS-positive, diastase-digestible material, probably glycogen granules, in their cytoplasm. A small number of reticulin fibers existed among the neoplastic cells.

Neoplastic cells in tumors induced by MT-R10 showed no reaction for keratin, alpha-1 antitrypsin, lysozyme, desmin, factor Ⅷ-related antigen or S-100 protein. In contrast, neoplastic cells exhibited a strong reaction for ALP (Fig. 44). Macrophages infiltrating in the tumors gave positive reactions for ACP and NSE, and reacted with MAB1435, whereas neoplastic cells did not react positively with these stainings (Figs. 45 and 46).

Ossifying areas were frequently found in all tumors induced by inoculating rats with MT-R2 and MT-R10. These areas were composed of mature osseous tissue containing osteoids and osteoblastic cells giving an appearance of osteosarcoma (Fig. 47). The osteoid tissue was eosinophilic and stained blue by the azan-Mallory method. Multiple metastatic nodules

were detected in the lungs of two out of four rats bearing tumors which had been induced by subcutaneous inoculation with MT-R10/10. The metastatic tumors were composed of round, undifferentiated cells with hyperchromatic nuclei, being occasionally mixed with osteoid tissue (Fig. 48). The tumor induced by MT-R10/10 was serially passaged up to the 10th generation in syngeneic rats. The transplanted tumors retained the original histologic features in all the generations examined.

Table 1. Cytologic characteristics of the parent cell line and CDDP-selected cell lines

Cell line	Cell shape	DT (hr)	Peak chromosomal number (range)	Histochemical staining			Cytologic function (%)		
				ACP	NSE	ALP	EA	EAC	LP
MT-P	polygonal and spindle	25.5	two peaks; 64,76 (32-100)	2+	2+	2+	20	11	10
MT-R2	polygonal and spindle	NE	NE	2+	2+	3+	NE	NE	NE
MT-R10	round	22.3	88 (46-105)	±	±	3+	<3	<3	<3

The data of MT-P (parent cell line) are quoted from Chapter 2. MT-R2 and MT-R10, capable of proliferating in the presence of 0.2 and 1.0 μg CDDP/ml, respectively. DT, doubling time in vitro; ACP, acid phosphatase; NSE, nonspecific esterase; ALP, alkaline phosphatase; EA, rosette formation for the Fc-receptor; EAC, rosette formation for the C3-receptor; LP, phagocytosis of latex particles; ±, negative or weak; 2+, moderate; 3+, strong; NE, not examined. Percentage of positive cells for the functional markers was calculated by counting 400 cells. MT-P and MT-R10 were incubated for 60 min at 37°C after latex particles were added to culture medium.

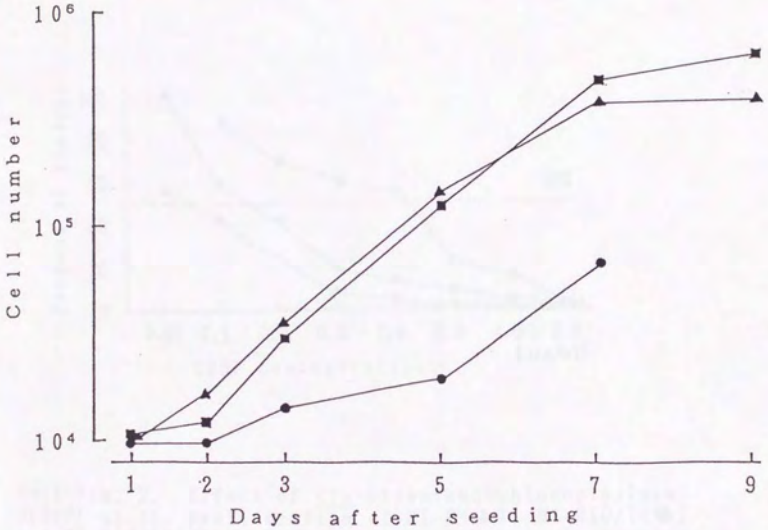

Text-Fig. 1. Growth curves of MT-P(▲), MT-R10/1(●) and MT-R10/10(■).

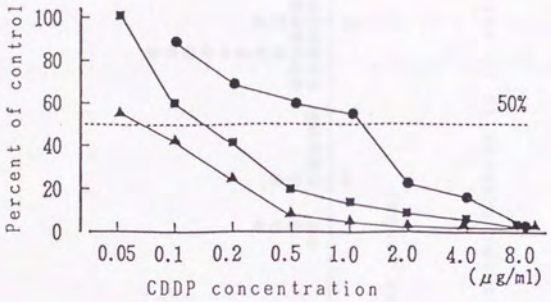

Text-Fig. 2. Effect of cis-Diamminedichloroplatinum (CDDP) on the proliferation of MT-P(▲), MT-R10/1(●) and MT-R10/10(■). Each point represents a percentage of viable cells at each concentration to control cells grown in CDDP-free medium. The numbers of control cells were 13.6 x 10^4 for MT-P, 1.5 x 10^4 for MT-R10/1 and 13.3 x 10^4 for MT-R10/10.

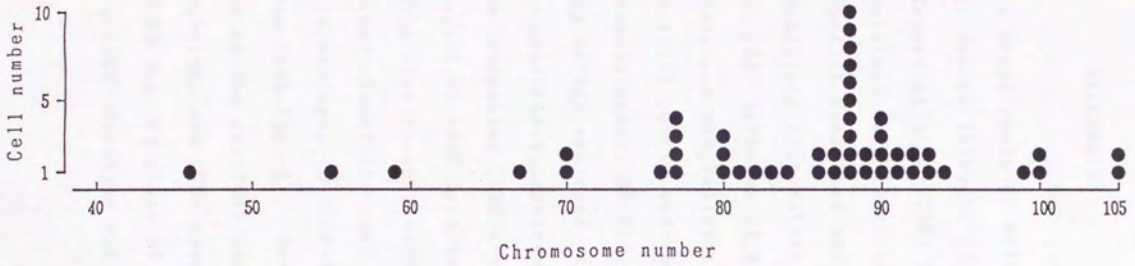

Text-Fig. 3. Distribution of chromosome numbers in 50 cells of MT-R10.

DISCUSSION

CDDP has a broad range of antitumor activity in human and animal tumors (Kikuchi et al., 1986; Kociba et al., 1970; Kuppen et al., 1988; Sorenson and Eastman, 1988). CDDP-resistant cell lines have been established from various types of human and animal tumors in order to study the mechanisms responsible for the induction of resistance to CDDP (Kikuchi et al., 1986; Kuppen et al., 1988; Sorenson and Eastman, 1988). However, the details are still poorly understood.

In the present study, MT-R10 cells capable of proliferating in the presence of 1.0 μg CDDP/ml were induced by continuous exposure of the parent cells, MT-P, to increasing CDDP concentrations. MT-R10 at passage 1 in CDDP-free medium (MT-R10/1) showed remarkably slow growth, whereas the same cell line regained almost the same growth ability as MT-P after 10 passages in CDDP-free medium (MT-R10/10) (see Text-Fig. 1). Because DNA has been implicated as the critical target for CDDP-induced cytotoxicity, and CDDP causes cells to become blocked at the G_2 phase of the cell cycle (Kuppen et al., 1988; Sorenson and Eastman, 1988),

MT-R10/1 might be in G_2 arrest. The 50% growth-inhibition concentration of CDDP was 15.3 times higher for MT-R10/1 and 2 times higher for MT-R10/10 than that for MT-P. Since MT-R10/10 was passaged 10 times in CDDP-free medium and proliferated better than did MT-R10/1, the difference in resistance to CDDP between the two cell lines may be due to their relative growth ability.

Monolayer cultures prepared from MT-R10 consisted of round, epithelial type cells arranged in a compact sheet, and the histiocytic characteristics observed in MT-P were no longer detectable in MT-R10 (see Table 1). The fine structure of MT-R10 cells was characterized by poorly developed cytoplasmic organelles, suggesting their undifferentiated and primitive nature. Moreover, the peak chromosomal number in MT-P differed from that in MT-R10. These observations suggest that MT-R10 may have been induced either by modification of MT-P or by selection from it as a result of the CDDP treatment. This remains to be clarified by further studies.

The tumors induced in rats by inoculation with MT-R10 had histologic features markedly different from those of MFH and MFH-MT. They consisted of small, round, undifferentiated cells with the scanty

cytoplasm and hyperchromatic nuclei. They showed an organoid or trabecular structure and neoplastic cells were often arranged in a compact sheet. Such structures have never been described in MFH. Although the storiform type of MFH is characterized by the presence of fibroblastic cells and collagenic fibers (Enjoji et al., 1980; Konishi et al., 1982; Stiller and Katenkamp, 1981), no such collagenic fibers were demonstrable in the induced tumors. Histiocytic lysosomal markers such as ACP, NSE, lysozyme, and alpha-1 antitrypsin as well as an antigenic marker demonstrable by MAB1435 were not detected in proliferating neoplastic cells. These histologic features were retained in serially transplanted tumors and in metastatic lesions in the lungs of syngeneic rats. Based on these findings, the tumors induced in rats by inoculation with MT-R10 seemed to be undifferentiated sarcoma.

Ultrastructurally, histiocytic, fibroblastic, and undifferentiated cells have been recognized as three major components of human and animal MFH (Maruyama et al., 1983; Holzhausen and Stiller, 1988). The origin of the three cell types in MFH is still controversial. Some workers (Roholl et al., 1986)

have suggested that a group of MFH is heterogeneous and probably derived from more than one progenitor cell. On the other hand, other workers (Konishi et al., 1982; Holzhausen and Stiller, 1988; Genberg et al., 1989) have advocated that both the histiocytic and fibroblastic cells constituting MFH may be derived from a common undifferentiated stem cell. More recently, it has been reported that histologic phenotypes reminiscent of leiomyosarcoma, osteosarcoma, schwannoma, and liposarcoma were mixed in parts of MFH (Brooks, 1986), and that xenografts of human MFH in nude mice showed leiomyogenic or schwannian differentiation (Roholl et al., 1988). In a study using monoclonal anti-human MFH antibodies, it was suggested that MFH and liposarcoma may have a common origin from perivascular mesenchymal cells, which may have potential for multidirectional differentiation (Iwasaki et al., 1987). MT-R10 appeared to consist solely of undifferentiated cells. Nevertheless, rats inoculated with this cell line developed undifferentiated sarcoma rather than MFH. This property was retained during 10 serial transplantations in the syngeneic rats examined. It would therefore be interesting to see if undifferentiated MT-R10 displays an ability to transform into histiocytes

and/or fibroblasts by further *in vitro* passages.

Osseous tissues were not involved in the original rat MFH, which arose from subcutaneous tissue of the head, and no bone-formation was detected in the original MFH and MFH-MT, which was serially transplanted subcutaneously in syngeneic rats up to the 45th generation (Chapter 1). It was noteworthy, therefore, that ossifying tissues were often found in tumors induced in rats by inoculation with MT-R10. The ossifying tissues have sporadically been observed in tumors developed at the tail-root or tumors induced by inoculating MT-P (Chapters 1 and 2). Histologically, the lesions appeared to be osteosarcomas consisting of a mixture of osteoblasts, osteoid tissue, and osseous tissue. Neoplastic cells constituting the lesions showed strong staining for ALP, as observed previously in human osteosarcomas (Yoshida *et al.*, 1988). These findings suggest that MT-R10 may have osteogenic potential. An undifferentiated mesenchymal cell has been surmised to be the progenitor cell of osteosarcoma (Yoshida *et al.*, 1988). Since osseous tissues have occasionally been observed in human and experimental rat MFH

(Brooks, 1986; Greaves et al., 1985), MFH and osteosarcoma may be derived from a common precursor cell. The mechanisms by which undifferentiated cells with osteogenic potential were induced by continuous exposure of cultured rat MFH (MT-P) to CDDP remain to be clarified.

SUMMARY

A cis-Diamminedichloroplatinum (CDDP)-selected cell line (MT-R10) was induced by continuous exposure of in vitro passaged cells (MT-P) established from a transplantable rat malignant fibrous histiocytoma (MFH-MT) to CDDP. MT-R10, capable of proliferating in the presence of 1.0 μg CDDP/ml, was passaged in CDDP-free medium. The doubling time of MT-R10 at passage 10 (MT-R10/10) was almost the same as that of MT-P, being 22.3 and 25.5 hr, respectively. The concentration of CDDP required for 50% inhibition of MT-R10/10 proliferation was twofold higher than that of MT-P. MT-R10 consisted of round, epithelial type cells arranged in a compact sheet. Ultrastructurally, MT-R10 cells had numerous free ribosomes, some mitochondria, and other poorly developed cytoplasmic organelles suggesting their undifferentiated nature. MT-R10 cells showed no reaction for acid phosphatase or nonspecific esterase. Tumors induced in syngeneic rats by inoculation with MT-R10 consisted of small, round, undifferentiated cells with the scanty cytoplasm. They showed organoid and trabecular patterns, and were often arranged in a compact sheet. The neoplastic

cells showed no reaction for any of the histiocytic lysosomal and antigenic markers tested, but exhibited a strong reaction for alkaline phosphatase. Bone-formation was often observed in the tumors. These observations suggest that CDDP-selected, undifferentiated cells may have osteogenic potential and may be one of the progenitor cells of MFH-MT.

CHAPTER 5

CHARACTERISTICS OF CLONED CELL LINES ESTABLISHED FROM A TRANSPLANTABLE RAT MALIGNANT FIBROUS HISTIOCYTOMA (MFH-MT)

INTRODUCTION

Malignant fibrous histiocytoma (MFH) consists of histiocytic and fibroblastic cells in varying proportions and is frequently mixed with xanthoma cells, multinucleated giant cells, and various types of inflammatory cells, showing a broad spectrum of histologic patterns (Enjoji et al., 1980; Stiller and Katenkamp, 1981). Based on enzyme/immunohistochemical and electron microscopic examinations, histiocytes (Hagari and Yumoto, 1987; O'Brien and Stout, 1964; Strauchen and Dimitriu-Bona, 1986), fibroblasts (Krawisz et al., 1981; Roholl et al., 1986) or undifferentiated mesenchymal cells (Holzhausen and Stiller, 1988; Roholl et al., 1986; Stiller and Katenkamp, 1981) have been presumed to be possible progenitor cells of MFH. However, relationship between these cells is still unclear.

In an attempt to clarify the histogenesis of MFH, neoplastic cell lines have been isolated from human MFH and examined in detail. As a result, neoplastic histiocytes with a potential for multidirectional differentiation have been proposed as the origin of MFH by Iwasaki et al.

(1982) and Shirasuna et al. (1985). On the other hand, Roholl et al. (1986) concluded that a group of MFH is heterogeneous and is probably derived from more than one progenitor cell. Iwasaki et al. (1987), in a subsequent study using monoclonal anti-MFH antibodies, reported that MFH has an origin from the perivascular mesenchymal cells having capability to form various types of cells.

In the foregoing chapters, the author demonstrated that a transplantable rat MFH (MFH-MT) established by him comprised cells having histiocytic markers and undifferentiated cells (MT-R10) with osteogenic potential. However, relationship between these two cell types and mechanisms by which various histologic patterns are induced by inoculation in rats with these cells still remain unanswered. In the present work, four neoplastic clones were isolated from in vitro passaged parent cells (MT-P) derived from MFH-MT and were examined by light and electron microscopy as well as enzyme/immunocytochemistry. In addition, tumors induced in rats by inoculating the cloned cells were examined histologically. It was expected that such studies will shed some light on the histogenesis of MFH. This chapter

describes the results obtained in these studies.

MATERIALS AND METHODS

Cell Culture: The derivation of MT-P from MFH-MT has been described in Chapter 2. MT-P at passage 21 were cloned twice consecutively by a limiting dilution technique as described (Iwasaki et al., 1987). Four cloned cell lines, MT-7, MT-8, MT-9, and MT-10, were established. Cloned cells were cultured in a humidified, 5% CO_2 atmosphere at 37℃. The growth medium used was Dulbecco's minimum essential medium (GIBCO, Grand Island, NY) supplemented with 10% fetal bovine serum (GIBCO), streptomycin (100 μg/ml), and penicillin (100 U/ml). Confluent cell sheets were subcultured by dispersing cells with a mixture of 0.1% trypsin and 0.02% ethylene-diaminetetraacetic acid in phosphate-buffered saline at 7- to 10-day intervals.

Observations of Cloned Cells: Growth of cloned cells was observed at passage level 5 as described for cell culture of MT-R10 in Chapter 4. The doubling time was determined by the cell numbers 2 and 5 days after seeding. Cells grown on tissue culture chamber slides (LAB-TEK, Miles, IL) were

fixed in Bouin's fluid or 4% formol calcium at 4℃ for 1-2 hr. They were examined morphologically and enzymecytochemically by the methods described in Chapters 2 and 4. For the indirect immunoperoxidase method, cells fixed in acetone were reacted with 100-fold-diluted anti-rat monocytes/macrophages monoclonal antibody (MAB1435) (Chemicon International Inc., CA) and 400-fold-diluted peroxidase-conjugated affinipure goat anti-mouse IgG, Fc fragment antibody (Jackson Immunoresearch Laboratories, Inc., PA) as secondary antibodies. Immunorosette formations for Fc- and C3-receptors, and phagocytic activities to latex particles or sheep red blood cells (SRBC) were examined by the conventional methods as described in Chapter 2.

For electron microscopy, cloned cells pelleted by centrifugation were processed and embedded in epoxy resin by the methods described in Chapter 2. Thin sections were stained with uranyl acetate and lead citrate and examined in a JEM-100B electron microscope at 80 kV.

In vivo Observations of Cloned Cells: One ml of a cell suspension containing 10^7 cloned cells at

passage levels 1, 7, and 21 was inoculated subcutaneously into syngeneic male F344 rats, 10-25 weeks old. The diameters of all tumors developed in inoculated sites were measured once weekly with calipers. Tumors developed by inoculating cloned cells at *in vitro* passage 7 were minced into small pieces, < 2 mm in diameter, with scissors and transplanted subcutaneously at the interscapular region of syngeneic male rats through a trocar with a diameter of 2 mm. Thereafter tumors were serially transplanted in syngeneic male rats when their diameter reached > 3 cm, about 5 to 6 weeks after transplantation.

Tumors removed from all the inoculated animals were weighed, processed, and examined morphologically and enzyme/immunohistochemically by the methods described for *in vivo* observations in the foregoing chapters.

RESULTS

Characteristics of *in vitro* Passaged Cloned Cells:
Text-Fig. 1 shows the growth curves of four cloned cell lines. The doubling times of MT-7, MT-8, MT-9, and MT-10 were 42.8, 27.7, 51.0, and 58.8 hr, respectively.

In monolayer cultures of the cloned cells stained with HE, each clone appeared to be composed of only one type of cells. Predominant cells of MT-7 were round or polygonal in shape with the abundant cytoplasm and a large round nucleus (Fig. 49). MT-8 consisted of elongated or spindle cells with a fusiform nucleus arranged in a fascicular pattern (Fig. 50). In MT-9 large, round cells with a lobulated nucleus were predominant (Fig. 51). Cells of MT-10 had the abundant cytoplasm with a few elongated cell processes and appeared dendritic in shape (Fig. 52). Cells of all the clones often contained a PAS-positive, diastase digestible material or oil red O-positive lipid droplets. Morphologic alterations were not observed during *in vitro* serial passages up to the 21st generation.

Ultrastructurally, cells of MT-7 and MT-10 resembled each other. They had the irregular surface

with many surface folds and their nuclei were oval or horseshoe-shaped. There were many lysosomes, slightly dilated rough-surfaced endoplasmic reticulum (RER), prominent Golgi complex, and some mitochondria in their cytoplasm (Figs. 53 and 54). The cytoplasm of occasional cells contained glycogen granules, lipid droplets, and phagosomes including cellular debris. MT-9 cells had many cytoplasmic extensions and indented nuclei. Their abundant cytoplasm possessed well-developed RER with dilated cisterna, prominent Golgi complex, many small lysosomes, and a moderate number of mitochondria (Fig. 55). Actin-like microfilament bundles with partly filamentous condensations were observed in about one-third of MT-9 cells examined (Figs. 55 and 56). Glycogen granules and lipid droplets were occasionally seen. MT-8 had the slightly irregular cell surface with some long cytoplasmic processes and a small oval nucleus. The cytoplasmic organelles were poorly developed, although there were numerous free ribosomes, a small number of lysosomes, some mitochondria, and glycogen granules (Figs. 57 and 58).

The results of enzyme/immunocytochemical and functional examinations on cloned cells are shown in

Table 1. MT-7, MT-9, and MT-10 reacted moderately or strongly for ACP (Fig. 59) and NSE. Positive reaction to MAB1435 in these clones appeared to correspond to the results for ACP and NSE (Fig. 60). In contrast, MT-8 reacted weakly to these stainings. MT-7, MT-8, and MT-9 gave a positive reaction for ALP (Fig. 61), while MT-10 did not. These staining properties were almost the same in all the passage levels examined. All the functional markers examined were small in percentage in all the cloned cell lines. No significant differences were observed in positive rates between the clones and between passage levels. The positive rates were 6 to 23% in rosette formation for the Fc-receptor (Fig. 62) and 2 to 7% in rosette formation for the C3-receptor. SRBC used for the Fc-receptor assay and latex particles were phagocytized by 3 to 19% and 3 to 8% after 60 min-incubation, respectively.

Histology of Tumors Induced in Rats by Inoculating Cloned Cells: Cells of four cloned cell lines at passage levels 1, 7, and 21 were inoculated subcutaneously into syngeneic rats. All the cloned cell lines were tumorigenic. Tumors became palpable two to three weeks

after inoculation and during following three to four weeks they developed into nodules ranging in diameter from 1.5 to 2.5 cm and in weight from 10 to 25 g. All tumors were well-circumscribed, multilobulated, and grayish in color. The tumors induced by MT-9 were firm masses with a fascicular structure on the cut surface, whereas those induced by the remaining clones were soft masses with several small cysts containing myxomatous liquid.

Tumors induced in syngeneic rats by four cloned cell lines were classified into four types according to the criteria of human MFH (Enjoji et al., 1980). The pleomorphic type was composed of round and pleomorphic cells, and a small amount of collagenic fibers (Fig. 63). These cells had the abundant cytoplasm and a pale nucleus with a prominent nucleolus. The myxoid type was composed of loosely arranged polygonal and round cells supported by alcian blue-positive material (Fig. 64), and occasionally contained giant cells with bizarre nuclei and hyaline globules. The globules stained red with PAS and were diastase resistant (Fig. 65). In myxoid areas cells containing oil red O-positive lipid droplets in their cytoplasm were frequently seen and appeared to be xanthomatous

cells (Fig. 66). The storiform type consisted predominantly of round histiocytic cells and elongated fibroblastic cells often arranged in a storiform or cartwheel pattern (Fig. 67). This type had a considerable amount of collagenic fibers among neoplastic cells. Tumors consisting mainly of spindle or fusiform cells arranged in an interlocking pattern or a compact sheet and containing no demonstrable collagenic fibers were referred to as the spindle-cell type in this paper (Fig. 68). In all the types neoplastic cells contained PAS-positive and diastase-digestible material, probably glycogen granules, and reticulin fibers demonstrable by the Watanabe's silver impregnation method were around neoplastic cells.

All four cloned cell lines produced tumors with a similar histologic pattern irrespective of their passage level (Table 2). Tumors induced by MT-7 and MT-10 were composed of a mixture of the pleomorphic, myxoid, and storiform types, and there was no distinct border between these types. Tumors induced by MT-9 consisted uniformly of the storiform type. Rats inoculated with MT-8 developed spindle-cell type tumors. Some parts of these tumors

contained the pleomorphic and myxoid types.

Enzyme/immunohistochemically, neoplastic cells constituting the pleomorphic, myxoid, and storiform types gave moderately or strongly positive reactions for ACP and NSE and reacted to MAB1435 (Fig. 69). In contrast, the spindle-cell type did not react to these stainings (Fig. 70). Tumors induced by MT-7, MT-8, and MT-9 reacted strongly for ALP, while those induced by MT-10 gave a faint reaction for ALP (Table 2). Positive reactions for alpha-1 antitrypsin, S-100 protein, and lysozyme (Fig. 71) were sporadically observed in all induced tumors. On the other hand, no positive reactions were demonstrated for factor Ⅷ-related antigen, keratin, and desmin in any of the tumors induced.

To investigate possible histologic variations that may occur during serial transplantation of tumors, the tumors induced by cloned cells were serially transplanted in syngeneic rats up to the 5th generation. The transplanted tumors from MT-9 retained histologic features of the storiform type throughout the generations examined. Transplants at the 2nd passage from MT-7 and MT-10 consisted of a mixture of the pleomorphic, myxoid, and storiform

types and bore a close resemblance to those of the 1st passage. In subsequent transplantations, however, spindle-cell areas consisting of undifferentiated cells made an appearance. In serial transplantation of the tumor induced by MT-8, the spindle-cell type became gradually predominant and it was accompanied with organoid structures in which small, round or fusiform cells with the scanty cytoplasm and hyperchromatic nuclei proliferated around vascular channels (Fig. 72). Neoplastic cells constituting storiform type-transplants from MT-9 gave positive reactions for ACP and NSE, whereas those of spindle-cell type-transplants from MT-7, MT-8, and MT-10 were negative for both enzymatic markers (Table 2). ALP was positive in transplants from all four cloned cell lines (Fig. 73) (Table 2). Osseous tissues consisting of osteoids, osteoblasts, and calcifying areas were sporadically observed in spindle-cell areas of transplants from MT-8 and MT-10 (Fig. 74).

Table 1. Results of enzyme/immunocytochemical and functional examinations on cloned cells established from a transplantable rat malignant fibrous histiocytoma (MFH-MT)

Clone	In vitro passage level	Staining				Cytological function (%)			
		ACP	NSE	ALP	MAB	EA	EAC	EA-P	L-P
MT-7	1 - 4	3+	3+	3+	2+	7	2	5	8
	12	3+	2+	2+	NE	NE	NE	NE	NE
	16 - 18	3+	2+	2+	NE	6	2	13	5
MT-8	1 - 4	1+	1+	2+	1+	23	7	19	3
	12	2+	1+	2+	NE	NE	NE	NE	NE
	16 - 18	1+	1+	2+	NE	10	2	11	7
MT-9	1 - 4	3+	2+	2+	2+	8	3	6	3
	12	3+	2+	3+	NE	NE	NE	NE	NE
	16 - 18	3+	3+	2+	NE	7	4	3	6
MT-10	1 - 4	3+	2+	-	3+	11	7	15	5
	12	3+	3+	-	NE	NE	NE	NE	NE
	16 - 18	3+	2+	-	NE	21	3	5	6

ACP:acid phosphatase, NSE:nonspecific esterase, ALP:alkaline phosphatase, MAB:anti-rat monocytes/macrophages monoclonal antibody, EA:rosette formation for the Fc-receptor, EAC: rosette formation for the C3-receptor, EA-P:phagocytosis of SRBC used for the Fc-receptor assay, L-P:phagocytosis of latex particles. -:negative, 1+:faint, 2+:moderate, 3+: strong, NE:not examined. Percentage of positive cells for functional markers was calculated by counting 400 cells.

Table 2. Enzyme/immunohistochemical findings of tumors induced in syngeneic rats by four cloned cell lines

Clone	Tumor type	Staining * ACP	NSE	ALP	MAB
MT-7	TC-1,TC-7,TC-21; pleomorphic, myxoid and storiform types	3+	2+	3+	2+
	#3, #5; spindle-cell type	-	-	3+	NE
MT-8	TC-1,TC-7,TC-21; spindle-cell type	-	-	3+	-
	#3, #5; spindle-cell type	-	-	3+	NE
MT-9	TC-1,TC-7,TC-21; storiform type	2+	2+	3+	3+
	#3, #5; storiform type	3+	3+	3+	NE
MT-10	TC-1,TC-7,TC-21; pleomorphic, myxoid and storiform types	2+	2+	1+	2+
	#3, #5; spindle-cell type	-	-	3+	NE

* See footnotes of Table 1. TC-1, TC-7 and TC-21 are tumors induced by cloned cells at 1, 7 and 21 passage levels, respectively. #3 and #5 are serial transplantation numbers of tumors induced by cloned cells at in vitro passage level 7.

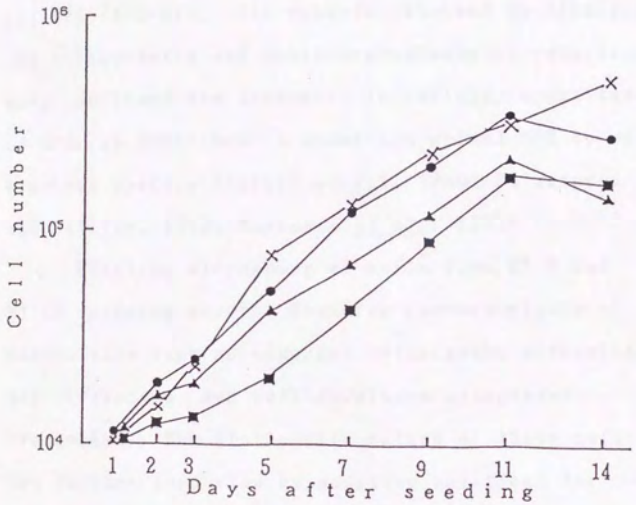

Text-Fig. 1. Growth curves of four cloned cell lines, MT-7(●), MT-8(×), MT-9(▲) and MT-10(■), established from a transplantable rat malignant fibrous histiocytoma (MFH-MT).

DISCUSSION

In the present study the author established four cloned neoplastic cell lines from a transplantable rat MFH (MFH-MT). The results obtained by examining the cloned cells and their transplants in syngeneic rats confirmed the diversity in cellular constituents of MFH, as described in human and animal MFH by many previous workers (Enjoji et al., 1980; Holzhausen and Stiller, 1988; Maruyama et al., 1983).

Electron microscopy of cells from MT-7 and MT-10 revealed several features characteristic of histiocytes such as numerous cytoplasmic extensions, many lysosomes, and well-developed cytoplasmic organelles. The histiocytic nature of these cells was further supported by positive reactions for ACP and NSE and by a positive reaction with MAB1435. Cells of MT-9 had similar ultrastructural and enzyme/immunocytochemical features to those of MT-7 and MT-10, but they contained microfilaments and well-developed dilated RER in their cytoplasm. Neoplastic cells forming human fibrosarcomas were characterized by smooth cytoplasmic membrane, elongated nuclei, and well-developed dilated RER, but lysosomes were

not observed in their cytoplasm (Nakahama et al., 1989). Fibroblasts having intracytoplasmic actin-like thin filaments were often observed in dermatogenic contracture and are known as myofibroblasts (Vande Berg et al., 1989). Fine structures of MT-9 cells suggested that they may be intermediate forms between histiocytes and fibroblasts. Such cells have occasionally been detected in human and animal MFH (Holzhausen and Stiller, 1988; Kato et al., 1990; Maruyama et al., 1983). Cells of MT-8 stained faintly positive for ACP and NSE and with MAB1435. These cells had the rather smooth cytoplasmic membrane and poorly developed cytoplasmic organelles and were interpreted as undifferentiated mesenchymal cells that have occasionally been seen in MFH (Holzhausen and Stiller, 1988; Maruyama et al., 1983; Roholl et al., 1986). The incidences of rosette formation and phagocytic activities were low in all the clones. This may be due to a lower differentiation stage of the cloned cells examined.

Cloned cells established from human MFH were polygonal in shape and exhibited histiocytic differentiation with positive reactions for lysosomal enzymes and high incidences of functional markers (Iwasaki et al.,

1982; Shirasuna et al., 1985). Roholl et al. (1986) isolated two cell lines each from a human MFH. In vitro neoplastic cells from the first MFH ultrastructurally resembled primitive mesenchymal cells and those from the second MFH resembled fibroblastic cells. The two lines did not exhibit immunorosetting and phagocytosis. These observations suggested heterogeneity of an MFH group.

All the clones were tumorigenic when inoculated subcutaneously into syngeneic rats and induced MFH with various histologic patterns. Tumors induced by MT-7 and MT-10 cells having a histiocytic appearance were of the pleomorphic, myxoid or storiform type. Cells of MT-9, a possible intermediate form between histiocyte and fibroblast, produced storiform type tumors containing a large amount of collagenic fibers, suggesting that the cells have capability to produce collagenic fibers during the tumor development. Fibrosarcomas are abundant in collagenic fibers. However, the histology of the storiform type differed from fibrosarcoma in that the latter consisted predominantly of neoplastic fibroblasts negative for lysosomal markers arranged in a herring-bone pattern (Nakahama et al., 1989). It has been

reported that some histiocytic cells underwent morphologic alteration into fibroblastic cells during a long-term cultivation and that neoplastic histiocytes in MFH may be able to behave as facultative fibroblasts under appropriate conditions (Hagari and Yumoto, 1987; Iwasaki et al., 1982; Kato et al., 1990; Shirasuna et al., 1985; Strauchen and Dimitriu-Bona, 1986).

Tumors induced by MT-8 were of the spindle-cell type consisting of undifferentiated cells negative for lysosomal markers, and were accompanied with organoid structures. These findings were in agreement with those of MT-R10 described in Chapter 4. These tumors appeared to be undifferentiated sarcomas. It is worth noting that transplants from MT-7 and MT-10 developed spindle-cell areas consisting of cells negative for lysosomal markers, as observed in the tumors induced by MT-8. Maruyama et al. (1983), in a study on rat MFH induced by 4-(hydroxyamino)quinoline 1-oxide, described that the population of undifferentiated cells increased as serial transplantation in syngeneic rats progressed. These observations suggest that cells forming MFH may dedifferentiate into undifferentiated cells.

Recent studies (Genberg et al., 1989; Greaves et al., 1985; Holzhausen and Stiller, 1988; Maruyama et al., 1983) seem to favor the hypothesis that the precursor of MFH is a primitive mesenchymal cell. Presumably, undifferentiated cells of MT-8 may be a precursor of cells with histiocytic nature capable of acting as facultative fibroblasts. Differences in morphology and reactivities to stainings for cytological markers between the clones may depend on different stages of cellular differentiation. However, it is still uncertain why inoculation of each clone having a homogeneous cell population into rats resulted in the development of an MFH with a pleomorphic pattern. This may be explained by assuming that each clone has capability to differentiate into various directions.

Osseous tissue has occasionally been found in human and experimental rat MFH (Brooks, 1986; Greaves et al., 1985). The similar lesions were observed in spindle-cell areas of transplants from MT-8 and MT-10 and tumors induced by MT-R10 (Chapter 4); the lesions were more frequently seen in tumors of MT-R10 than in those of MT-8 and MT-10. It has recently been reported in a study using monoclonal

anti-MFH antibodies that MFH and liposarcoma have a common origin from the perivascular mesenchymal cells (Iwasaki et al., 1987). Moreover, xenografts of human MFH in nude mice have been shown to express leiomyogenic or schwannian differentiation (Roholl et al., 1988). MFH may be originated from a pluripotential progenitor for mesenchymal differentiation (Brooks, 1986). The cloned cell lines the author established and transplantable MFH induced by the clones may provide useful experimental systems for studying the histogenesis and growth behavior of this tumor.

SUMMARY

Four cloned cell lines, MT-7, MT-8, MT-9, and MT-10, were established from a transplantable malignant fibrous histiocytoma (MFH-MT) of F344 rats to investigate the histogenesis of the tumor. Cells of MT-7, MT-9, and MT-10 had fine structures characteristic of histiocytes such as numerous cell processes, many lysosomes, and well-developed cytoplasmic organelles. They stained positively for histiocytic lysosomal markers of acid phosphatase (ACP) and nonspecific esterase (NSE), and reacted with anti-rat monocytes/macrophages monoclonal antibody (MAB1435). In addition, MT-9 cells contained microfilaments and well-developed rough-surfaced endoplasmic reticulum in their cytoplasm, suggesting MT-9 cells may be facultative fibroblasts. MT-8 cells stained weakly for ACP and NSE and with MAB1435 and had scant cytoplasmic organelles. They were identified as undifferentiated mesenchymal cells. All the clones were tumorigenic when inoculated into syngeneic rats. The tumors induced by inoculating MT-7 or MT-10 consisted of a mixture of the pleomorphic, myxoid, and storiform types of MFH, and those by

MT-9 were of the storiform type. Cells forming these tumors stained positively for ACP and NSE, and reacted with MAB1435. Tumors induced by MT-8 consisted of undifferentiated cells negative to these stainings. During serial transplantation in rats of these tumors, undifferentiated cells appeared in transplants from MT-7 and MT-10. Osseous tissues sporadically developed in areas consisting of undifferentiated cells. Based on these observations, the histogenesis of malignant fibrous histiocytomas is surmised to be related to various differentiation stages shifting from pluripotential undifferentiated cells to histiocytic cells capable of acting as facultative fibroblasts.

CONCLUSIONS

Malignant fibrous histiocytoma (MFH) is a sarcoma consisting predominantly of fibroblastic and histiocytic cells often arranged in a storiform pattern and shows a great histologic diversity. Human MFH has been classified into the storiform, pleomorphic, myxoid, xanthogranulomatous (inflammatory), and giant cell types. The histogenesis of MFH is still debatable, although histiocytes, fibroblasts or undifferentiated cells have been surmised to be possible progenitor cells. The author succeeded in the serial transplantation of a spontaneous rat MFH in syngeneic rats. In an attempt to clarify the histogenesis of MFH, the transplantable tumor line and cells cultivated from the tumor line were pathologically scrutinized. The results thus obtained led the author to the following conclusions:

1. A spontaneous MFH was found in subcutaneous tissue of the head of a 15-month-old male F344/DuCrj rat. The tumor was serially transplanted in subcutaneous tissue of syngeneic rats up to the 45th generation. The transplantable tumor was designated MFH-MT.

2. The original tumor and MFH-MT were composed of a mixture of fibroblastic and histiocytic cells arranged in a storiform pattern and diagnosed as the storiform type. On the other hand, tumors developed in the lungs and cutaneous tissues of the tail-root of rats by transplantation and tumors heterotransplanted into athymic nude mice had a mixed histologic structure of the storiform, pleomorphic, myxoid, and giant cell types. Moreover, sclerosing hemangioma-like and osteosarcoma-like structures were observed. These observations revealed that MFH-MT has a wide range of histologic patterns, as have been reported in human MFH.

3. The growth of MFH-MT transplanted in rats was significantly retarded by two antitumor drugs, adriamycin and cis-Diamminedichloroplatinum (CDDP). The retarded tumors consisted predominantly of fibroblastic cells and abundant collagenic fibers. This suggested that MFH-MT comprised cell types differing in susceptibility to the antitumor drugs tested.

4. In vitro passaged cells (MT-P) derived from MFH-MT

were examined morphologically and functionally. MT-P contained polygonal cells having numerous cell processes and many lysosomes in their cytoplasm, and the cells reacted positively for acid phosphatase (ACP), nonspecific esterase (NSE), and alkaline phosphatase. Immunorosette formations for Fc- and C3-surface receptors and phagocytic activity were demonstrated in 10-20% of MT-P. Tumors induced in rats by inoculating MT-P showed variable histologic patterns. These observations suggest that MFH-MT is heterogeneous, and some cells constituting MFH-MT have histiocytic markers.

5. Histochemical stainings in combination with various enzymes demonstrated that glycosaminoglycans (GAG) existing in myxoid areas of MFH-MT contained both chondroitin sulfate and hyaluronic acid (HA). In cellulose acetate electrophoresis, bands of GAG, which had been isolated from cyst-fluid of MFH-MT and from culture medium of MT-P, corresponded to those of the standard HA. These results suggest that neoplastic cells forming MFH-MT may be at an embryonal and undifferentiated stage.

6. A CDDP-selected cell line (MT-R10) capable of proliferating in the presence of 1.0 μg CDDP/ml was induced from MT-P. MT-R10 cells failed to reveal histiocytic markers, which were observed in MT-P, and ultrastructurally, MT-R10 cells had poorly developed cytoplasmic organelles suggesting their undifferentiated nature. Tumors induced in rats by inoculating MT-R10 showed organoid and trabecular structures formed by undifferentiated cells negative for lysosomal enzymatic markers, and osteosarcomatous lesions were frequently observed in the tumors. It is suggested from these findings that undifferentiated cells with osteogenic potential are comprised in MFH-MT.

7. Four cloned cell lines, MT-7, MT-8, MT-9, and MT-10, were established from MT-P and examined morphologically and enzyme/immunocytochemically. MT-7 and MT-8 reacted positively for ACP and NSE and with anti-rat monocytes/macrophages monoclonal antibody (MAB1435) and showed fine structures characteristic of histiocytes. Tumors induced in rats by inoculating both lines consisted of a mixture of the pleomorphic, myxoid, and storiform

types, and in subsequent transplantations undifferentiated cells made an appearance, suggesting neoplastic cells may dedifferentiate into undifferentiated cells. MT-9 cells appeared to be an intermediate form between histiocytes and fibroblasts. Tumors induced by MT-9 had uniform histology of the storiform type including a large amount of collagenic fibers. MT-9 cells were regarded as facultative fibroblasts. MT-8 cells had scant cytoplasmic organelles, and tumors induced by MT-8 consisted of cells negative for histiocytic markers and were diagnosed as undifferentiated sarcomas. MT-8 cells were interpreted as undifferentiated mesenchymal cells.

8. On the basis of the results obtained in a series of studies, MFH was deemed to manifest diverse histologic patterns depending on different differential stages of neoplastic cells shifting from pluripotential undifferentiated cells to histiocytic cells capable of acting as facultative fibroblasts. MFH-MT seemed to be a useful experimental system for further studies on the histogenesis and growth behavior of MFH.

ACKNOWLEDGMENTS

The author wishes to express his sincere appreciation and gratitude to Dr. Masanori Tajima, Director of Nippon Institute for Biological Science, for his cordial support as well as kind help in the studies as a coworker and critical review of the thesis, and Dr. Naoaki Goto, Professor of Department of Veterinary Pathology, Faculty of Agriculture, the University of Tokyo, for his kind direction and consistent encouragement during the preparation of the thesis.

The author appreciates Messrs. Masaharu Togo, Toshiki Saitoh, Kazumoto Shibuya and Satoru Kudow, and Mmes. Miheko Ihara and Nobuko Shibuya in author's Institute for their cooperation and valuable discussion. Thanks are also due to Messrs. Yoshisada Ogata, Mitsuo Kaneko and Shinobu Ishikawa in author's Institute for their excellent technical assistance during the course of this work.

REFERENCES

Angello, J. C., Danielson, K. G., Anderson, L. W., and Hosick, H. L. 1982. Glycosaminoglycan synthesis by subpopulations of epithelial cells from a mammary adenocarcinoma. Cancer Res. 42: 2207-2210.

Becker, M., Moczar, M., Poupon, M. F., and Moczar, E. 1986. Solubilization and degradation of extracellular matrix by various metastatic cell lines derived from a rat rhabdomyosarcoma. J. Natl. Cancer Inst. 77: 417-424.

Brooks, J. J. 1986. The significance of double phenotypic patterns and markers in human sarcomas. A new model of mesenchymal differentiation. Am. J. Pathol. 125: 113-123.

Brown, D. G., Johnson, N. F., and Wagner, M. M. F. 1985. Multipotential behaviour of cloned rat mesothelioma cells with epithelial phenotype. Br. J. Cancer. 51: 245-252.

Chiarugi, V. P., Vannucchi, S., Cella, C., Fibbi, G., Rosso, M. D., and Cappelletti, R. 1978. Intercellular glycosaminoglycans in normal and neoplastic tissues. Cancer Res. 38: 4717-4721.

Chiu, B., Churg, A., Tengblad, A., Pearce, R., and McCaughey, W. T. E. 1984. Analysis of hyaluronic acid in the diagnosis of malignant mesothelioma. Cancer. 54: 2195-2199.

Di Marco, A., Gaetani, M., and Scarpinato, B. 1969. Adriamycin (NSC-123,127). A new antibiotic with antitumor activity. Cancer Chemother. Rep. 53: 33-37.

Du Boulay, C. E. H. 1985. Immunohistochemistry of soft tissue tumors. A review. J. Pathol. 146: 77-94.

Enjoji, M., Hashimoto, H., Tsuneyoshi, M., and Iwasaki, H. 1980. Malignant fibrous histiocytoma. A clinicopathologic study of 130 cases. Acta Pathol. Jpn. 30: 727-741.

Fujimaki, Y., Sugiyama, M., and Isoda, M. 1985. Malignant fibrous histiocytoma in a fox. Jpn. J. Vet. Sci. 47: 147-150.

Garma-Aviña, A. 1987. Malignant fibrous histiocytoma of the giant cell type in a cat. J. Comp. Pathol. 97: 551-557.

Genberg, M., Mark, J., Hakelius, L., Ericsson, J., and Nister, M. 1989. Origin and relationship between different cell types in malignant fibrous histiocytoma. Am. J. Pathol. 135: 1185-1196.

Gleiser, C. A. and Carey, K. D. 1983. Malignant fibrous histiocytoma in a baboon. Lab. Anim. Sci. 33: 380-381.

Gleiser, C. A., Raulston, G. L., Jardine, J. H., and Gray, K. N. 1979. Malignant fibrous histiocytoma in dogs and cats. Vet. Pathol. 16: 199-208.

Gordon, M. Y., Riley, G. P., Watt, S. M., and Greaves, M. F. 1987. Compartmentalization of a haematopoietic growth factor (GM-CSF) by glycosaminoglycans in the bone marrow microenvironment. Nature (Lond.) 326: 403-405.

Greaves, P., Martin, J. M., and Masson, M. T. 1982. Spontaneous rat malignant tumors of fibrohistiocytic origin. An ultrastructural study. Vet. Pathol. 19: 497-505.

Greaves, P., Martin, J. M., and Rabemampianina, Y. 1985. Malignant fibrous histiocytoma in rats at sites of implanted millipore filters. Am. J. Pathol. 120: 207-214.

Hagari, Y. and Yumoto, T. 1987. Experimental tumors of myxoid malignant fibrous histiocytoma and hyaluronic acid production. Acta Pathol. Jpn. 37: 975-988.

Holzhausen, H. J. and Stiller, D. 1988. Cellular differentiations of storiform-pleomorphic malignant fibrous histiocytoma. An electron microscopic study on the histogenesis. Zentralbl. Allg. Pathol. 134: 363-381.

Inoue, A., Aozasa, K., Tsujimoto, M., Tamai, M., Chatani, F., and Ueno, H. 1984. Immunohistological study on malignant fibrous histiocytoma. Acta Pathol. Jpn. 34: 759-765.

Iwasaki, H., Isayama, T., Johzaki, H., and Kikuchi, M. 1987. Malignant fibrous histiocytoma. Evidence of perivascular mesenchymal cell origin. Immunocytochemical studies with monoclonal anti-MFH antibodies. Am. J. Pathol. 128: 528-537.

Iwasaki, H., Kikuchi, M., Takii, M., and Enjoji, M. 1982. Benign and malignant fibrous histiocytomas of the soft tissues. Functional characterization of the cultured cells. Cancer. 50: 520-530.

Kato, T., Takeya, M., Takagi, K., and Takahashi, K. 1990. Chemically induced transplantable malignant fibrous histiocytoma of the rat. Analyses with immunohistochemistry, immunoelectron microscopy and (^{3}H) thymidine autoradiography. Lab. Invest. 62: 635-645.

Kay, S. 1985. Angiomatoid malignant fibrous histiocytoma. Arch. Pathol. Lab. Med. 109: 934-937.

Kikuchi, Y., Miyauchi, M., Kizawa, I., Oomori, K., and Kato, K. 1986. Establishment of a cisplatin-resistant human ovarian cancer cell line. J. Natl. Cancer Inst. 77: 1181-1185.

Kociba, R. J., Sleight, S. D., and Rosenberg, B. 1970. Inhibition of dunning ascitic leukemia and walker 256 carcinosarcoma with cis-Diamminedichloroplatinum (NSC-119875). Cancer Chemother. Rep. 54: 325-328.

Konishi, Y., Maruyama, H., Mii, Y., Miyauchi, Y., Yokose, Y., and Masuhara, K. 1982. Malignant fibrous histiocytomas induced by 4-(hydroxyamino) quinoline 1-oxide in rats. J. Natl. Cancer Inst. 68:859-865.

Krawisz, B. R., Florine, D. L., and Scott, R. E. 1981. Differentiation of fibroblast-like cells into macrophages. Cancer Res. 41: 2891-2899.

Kuppen, P. J. K., Schuitemaker, H., van't Veer, L. J., de Bruijn, E. A., van Oosterom, A. T., and Schrier, P. I. 1988. Cis-Diamminedichloroplatinum(II)-resistant sublines derived from two human ovarian tumor cell lines. Cancer Res. 48: 3355-3359.

Le Douarin, N. M. 1984. Cell migrations in embryos. Cell. 38: 353-360.

Maekawa, A., Kurokawa, Y., Takahashi, M., Tokubo, T., Ogiu, T., Onodera, H., Tanigawa, H., Ohno, Y., Furukawa, F., and Hayashi, Y. 1983. Spontaneous tumors in F344/DuCrj rats. Gann. 74: 365-372.

Maruyama, H., Mii, Y., Emi, Y., Masuda, S., Miyauchi, Y., Masuhara, K., and Konishi, Y. 1983. Experimental studies on malignant fibrous histiocytomas. Ⅱ. Ultrastructure of malignant fibrous histiocytomas induced by 4-(hydroxyamino)quinoline 1-oxide in rats. Lab. Invest. 48: 187-198.

Nakahama, M., Takanashi, R., Yamazaki, I., and Machinami, R. 1989. Primary fibrosarcoma of the liver. Immunohistochemical and electron microscopic studies. Acta Pathol. Jpn. 39: 814-820.

Nakanishi, S. and Hizawa, K. 1984. Enzyme histochemical observation of fibrohistiocytic tumors. Acta Pathol. Jpn. 34: 1003-1016.

O'Brien, J. E. and Stout, A. P. 1964. Malignant fibrous xanthomas. Cancer 17: 1445-1455.

Palmer, T. E. and Monlux, A. W. 1979. Acid mucopolysaccharides in mammary tumors of dogs. Vet. Pathol. 16: 493-509.

Prehm, P. 1984. Hyaluronate is synthesized at plasma membranes. Biochem. J. 220: 597-600.

Renlund, R. C. and Pritzker, K. P. H. 1984. Malignant fibrous histiocytoma involving the digit in a cat. Vet. Pathol. 21: 442-444.

Roholl, P. J. M., Kleyne, J., Elbers, H., van DerVegt, M. C. D., Albus-Lutter, C. H., and van Unnik, J. A. M. 1985a. Characterization of tumour cells in malignant fibrous histiocytomas and other soft tissue tumours in comparison with malignant histiocytes. I. Immunohistochemical study on paraffin sections. J. Pathol. 147: 87-95.

Roholl, P. J. M., Kleyne, J., van Blokland, M., Spies, P. L., Rutgers, D. H., Albus-Lutter, C. E., and van Unnik, J. A. M. 1986. Characterization of two cell lines, derived from two malignant fibrous histiocytomas. J. Pathol. 150: 103-112.

Roholl, P. J. M., Kleyne, J., and van Unnik, J. A. M. 1985b. Characterization of tumor cells in malignant fibrous histiocytomas and other soft tissue tumors, in comparison with malignant histiocytes. Ⅱ. Immunoperoxidase study on cryostat sections. Am. J. Pathol. 121: 269-274.

Roholl, P. J. M., Rutgers, D. H., Rademakers, L. H. P. M., De Weger, R. A., Elbers, J. R. J., and van Unnik, J. A. M. 1988. Characterization of human soft tissue sarcomas in nude mice. Evidence for histogenic properties of malignant fibrous histiocytomas. Am. J. Pathol. 131: 559-568.

Satake, T. and Matsuyama, M. 1988. Cytologic features of ascites in malignant fibrous histiocytoma of the colon. Acta Pathol. Jpn. 38: 921-928.

Shibata, M., Izumi, K., Sano, N., Akagi, A., and Otsuka, H. 1989. Induction of soft tissue tumours in F344 rats by subcutaneous, intramuscular, intra-articular, and retroperitoneal injection of nickel sulphide (Ni_3S_2). J. Pathol. 157: 263-274.

Shibuya. H., Azumi, N., Onda, Y., and Abe, F. 1985. Multiple primary malignant fibrous histiocytoma of the stomach and small intestine. Acta Pathol. Jpn. 35: 157-164.

Shirasuna, K., Sugiyama, M., and Miyazaki, T. 1985. Establishment and characterization of neoplastic cells from a malignant fibrous histiocytoma. A possible stem cell line. Cancer 55: 2521-2532.

Singley, C. T. and Solursh, M. 1981. The spatial distribution of hyaluronic acid and mesenchymal condensation in the embryonic chick wing. Develop. Biol. 84: 102-120.

Skavlen, P. A., Speers, W. C., Peterson, R. R., Stevens, J. O., and Reite, M. L. 1988. Malignant fibrous histiocytoma in a bonnet macaque (Macaca radiata). Lab. Anim. Sci. 38: 310-311.

Solleveld, H. A., Haseman, J. K., and McConnell, E. E. 1984. Natural history of body weight gain, survival, and neoplasia in the F344 rat. J. Natl. Cancer Inst. 72: 929-940.

Sorenson, C. M. and Eastman, A. 1988. Mechanism of cis-Diamminedichloroplatinum(Ⅱ)-induced cytotoxicity. Role of G_2 arrest and DNA double-strand breaks. Cancer Res. 48: 4484-4488.

Stiller, D. and Katenkamp, D. 1981. Structural variability of malignant fibrous histiocytomas of soft tissue. Zentralbl. Allg. Pathol. 125: 369-380.

Stiller, D. and Katenkamp, D. 1983. Malignant fibrous histiocytoma of bone. Clinical pathology and histological diagnosis. Zentralbl. Allg. Pathol. 128: 5-20.

Strauchen, J. A. and Dimitriu-Bona, A. 1986. Malignant fibrous histiocytoma. Expression of monocyte/macrophage differentiation antigens detected with monoclonal antibodies. Am. J. Pathol. 124: 303-309.

Takaki, Y., Kishikawa, M., Sekine, I., Nishimori, I., Hirata, M., and Namiki, H. 1983. Primary malignant fibrous histiocytoma of the endometrium. Acta Pathol. Jpn. 33: 823-829.

Tanaka, H., Mori, Y., and Akedo, H. 1982. Histiocytic differentiation of mouse malignant fibrous histioctoma-like tumor cells by culturing with sodium butyrate. Cell Biol. International Rep. 6: 85-90.

Tanaka, T., Saito, R., Kajiwara, M., Soh, S., Hashimoto, K., and Yumoto, T. 1982. Fibrous histiocytoma of the nasal cavity and maxillary sinus. Acta Pathol. Jpn. 32: 657-669.

Tanimoto, T., Ohtsuki, Y., Sonobe, H., Takahashi, R., and Nomura, Y. 1988. Malignant fibrous histiocytoma in the spleen of a pig. Vet. Pathol. 25: 330-332.

Tanino, M., Odashima, S., Sugiura, H., Matsue, T., Kajikawa, M., and Maeda, S. 1985. Malignant fibrous histiocytoma of the lung. Acta Pathol. Jpn. 35: 945-950.

Vande Berg, J. S., Rudolph, R., Poolman, W. L., and Disharoon, D. R. 1989. Comparative growth dynamics and actin concentration between cultured human myofibroblasts from granulating wounds and dermal fibroblasts from normal skin. Lab. Invest. 61: 532-538.

Vannucchi, S. and Chiarugi, V. P. 1976. Surface exposure of glycosaminoglycans in resting, growing and virus transformed 3T3 cells. J. Cell Physiol. 90: 503-510.

Wagner, J. C., Munday, D. E., and Harington, J. S. 1962. Histochemical demonstration of hyaluronic acid in pleural mesotheliomas. J. Pathol. Bact. 84: 73-78.

Ward, J. M., Kulwich, B. A., Reznik, G., and Berman, J. J. 1981. Malignant fibrous histiocytoma. An unusual neoplasm of soft-tissue origin in the rat that is different from the human counterpart. Arch Pathol. Lab. Med. 105: 313-316.

Yamamoto, H. and Fujishiro, K. 1989. Pathology of spontaneous malignant fibrous histiocytoma in a Japanese white rabbit. Exp. Anim. (Tokyo) 38: 165-169.

Yoshida, H., Adachi, H., Hamada, Y., Aki, T., Yumoto, T., Morimoto, K., and Orido, T. 1988. Osteosarcoma. Ultrastructural and immunohistochemical studies on alkaline phosphatase-positve tumor cells constituting a variety of histologic types. Acta Pathol. Jpn. 38: 325-338.

Yumoto, T. and Morimoto, K. 1980. Experimental approach to fibrous histiocytoma. Acta Pathol. Jpn. 30: 767-778.

FIGURE LEGENDS

Fig. 1. Original tumor developed in subcutaneous tissue of the head of a male F344 rat. The cut surface of the tumor shows fascicular structure and is bloody. Bar=0.5 cm.

Fig. 2. A portion of the original tumor consisting of spindle cells and round cells arranged in a storiform pattern. HE, x 180.

Fig. 3. A transplantable tumor (MFH-MT) at the 11th generation grown at subcutaneous transplantation site in a syngeneic rat. Bar=1 cm.

Fig. 4. Electron micrograph showing fibroblastic cells in MFH-MT. The cells are spindle in shape and have dilated rough-surfaced endoplasmic reticulum and a moderate number of mitochondria in their cytoplasm. x 4,000.

Fig. 5. Electron micrograph showing histiocytic cells (H) and a fibroblastic cell (F) in MFH-MT. The histiocytic cells have well-developed

cytoplasmic organelles and a small number of lysosomes. x 4,000.

Fig. 6. A moderate reaction for acid phosphatase expressing coarse intracytoplasmic granules in MFH-MT cells. Gomori's method, x 300.

Fig. 7. Neoplastic cells in MFH-MT with a storiform pattern showing a faintly positive reaction for alpha-1 antitrypsin (arrows). PAP method, counterstained with hematoxylin, x 400.

Fig. 8. Tumor tissue of MFH-MT with a storiform pattern showing a positive reaction for alkaline phosphatase. Naphthol AS acetate method, x 250.

Fig. 9. A portion of myxoid area of MFH-MT developed in cutaneous tissue of the tail-root of a rat. Polygonal and round cells are loosely arranged and supported by myxomatous matrix. HE, x 250.

Fig. 10. MFH-MT transplanted in the lung of a rat showing an area containing many giant cells. HE, x 300.

Fig. 11. A portion of osteosarcoma-like structure in MFH-MT transplanted in the tail-root of a rat. HE, x 200.

Fig. 12. Part of MFH-MT transplanted in the lung of a rat showing elongated cells arranged in an interlocking pattern. HE, x 280.

Fig. 13. Part of MFH-MT transplanted in the lung of a rat showing sclerosing hemangioma-like structure. HE, x 120.

Fig. 14. Elongated cells in MFH-MT transplanted in the lung of a rat showing a positive reaction for S-100 protein (arrow). PAP method, counterstained with hematoxylin, x 350.

Fig. 15. MFH-MT heterotransplanted into a CRJ:CD-1 (ICR)-nu/nu mouse. Bar=1 cm.

Fig. 16. The cut surface of MFH-MT heterotransplanted to a nude mouse showing a watery appearance. Bar=0.5 cm.

Fig. 17. Pleomorphic cell area of MFH-MT transplanted

into a nude mouse. A strongly positive reaction for alpha-1 antitrypsin representing coarse intracytoplasmic granules in neoplastic cells. PAP method, counterstained with hematoxylin, x 300.

Fig. 18. MFH-MT transplanted to a rat treated with cis-Diamminedichloroplatinum. The tumor consists of fibroblastic cells and abundant collagenic fibers. Histiocytic cells are not seen. HE, x 250.

Fig. 19. Spindle, polygonal, and giant cell types seen in in vitro passaged cells (MT-P) derived from MFH-MT. HE, x 250.

Fig. 20. Electron micrograph of MT-P showing polygonal (P) and spindle cells (S). Glycogen granules (asterisk) and a phagosome (arrow) are seen. x 2,000.

Fig. 21. MT-P showing a positive reaction for acid phosphatase recognizable as perinuclear granules. Gomori's method, x 500.

Fig. 22. MT-P showing a perinuclear positive reaction for nonspecific esterase. Alpha-naphthyl acetate method, x 500.

Fig. 23. Latex particles phagocytized by MT-P. x 450.

Fig. 24. Part of a tumor developed in a rat inoculated with MT-P consisting of round and fusiform histiocytic cells. HE, x 200.

Fig. 25. PAS-positive, diastase-digestible material contained in histiocytic cells in a subcutaneous tumor of a rat induced by inoculating MT-P. PAS stain, x 250.

Fig. 26. Part of a tumor developed in a rat inoculated with MT-P showing fibroblastic cells arranged in a storiform pattern. HE, x 200.

Fig. 27. Part of a tumor developed in a rat inoculated with MT-P consisting of fibroblastic cells supported by myxomatous matrix. HE, x 200.

Fig. 28. Ossifying tissue in a tumor developed in a rat inoculated with MT-P consisting of osteoblasts, osteoid tissue, and calcifying areas. HE, x 120.

Fig. 29. A portion of a tumor developed in a rat

inoculated with MT-P showing a moderate reaction for nonspecific esterase. Alpha-naphthyl acetate method, x 240.

Fig. 30. Part of a tumor developed in a rat inoculated with MT-P showing a moderate reaction for alkaline phosphatase. Naphthol AS method, x 200.

Fig. 31. Part of a myxoid area of MFH-MT developed at the tail-root of a rat. The matrix stains positively with alcian blue. Alcian blue (pH 2.5) and nuclear fast red, x 180.

Fig. 32. Part of a myxoid area of the same MFH-MT as that shown in Fig. 31. Alcian blue-positive material has been completely digested by bovine hyaluronidase. Alcian blue (pH 2.5) and nuclear fast red after treating with bovine hyaluronidase, x 180.

Fig. 33. Cellulose acetate electrophoresis of glycosaminoglycans in cyst-fluid. S, start; 1 (C42-3) and 2 (C42-2), samples of cyst-fluid from MFH-MT; 3, standard heparin (HeP); 4, standard

chondroitin sulfate C (ChS-C); 5, standard chondroitin sulfate B (dermatan sulfate: DS); 6, standard chondroitin sulfate A (ChS-A); 7, standard keratan sulfate (KS); 8, standard hyaluronic acid (HA). The bands of lanes 1 and 2 appear to correspond to that of lane 8.

Fig. 34. Cellulose acetate electrophoresis of glycosaminoglycans in culture medium. S, start; 1, culture medium harvested 5 days after seeding of MT-P (TC-5); 2, culture medium harvested 13 days after seeding of MT-P (TC-13); 3, culture medium incubated for 5 days in the absence of MT-P (TC-C); 4, HeP; 5, DS; 6, ChS-A; 7, KS; 8, HA. The bands of lanes 1 and 2 apparently correspond to that of lane 8, whereas the corresponding band is absent in lane 3. See abbreviations in Fig. 33.

Fig. 35. Cellulose acetate electrophoresis of glycosaminoglycans treated with streptomyces hyaluronidase (SH). S, start; 1, ChS-A + SH; 2, HA + SH; 3, TC-13 + SH; 4, C42-3 + SH; 5, ChS-A; 6, HA; 7, TC-13; 8, C42-3. Although part of the band of lane 4, which slightly migrates

toward the positive electrode, faintly appears, bands of lanes 2, 3, and 4 are missing by SH treatment in contrast to those of no treated samples in lanes 6, 7, and 8, respectively. The band of lane 1 appears similar to that of lane 5, indicating that ChS-A is not digested by SH. See abbreviations in Figs. 33 and 34.

Fig. 36. Cis-Diamminedichloroplatinum (CDDP)-selected cells (MT-R10) capable of proliferating in the presence of 1.0 μg CDDP/ml. The cells appear round, epithelial type and are arranged in a compact sheet. HE, x 200.

Fig. 37. Electron micrograph of MT-R10. The cells appear dark and the cytoplasm contains numerous free ribosomes and some mitochondria with dark matrix. The other cytoplasmic organelles are poorly developed. x 6,800.

Fig. 38. Tumor induced in a rat by inoculating cells (MT-R2) capable of proliferating in the presence of 0.2 μg CDDP/ml. The tumor consists of fibroblastic and histiocytic cells as well as

a moderate amount of collagenic fibers arranged in a storiform pattern. HE, x 100.

Fig. 39. Tumor induced in a rat by inoculating MT-R2. Polygonal and round cells are loosely arranged and supported by myxoid matrix. HE, x 120.

Fig. 40. Tumor induced in a rat by inoculating MT-R2. A storiform pattern consists of fibroblastic cells and histiocytic cells moderately reactive for nonspecific esterase. Alpha-naphthyl acetate method, x 150.

Fig. 41. Tumor induced in a rat by inoculating MT-R10. Small, round, undifferentiated cells are arranged in a compact sheet. HE, x 140.

Fig. 42. Tumor induced in a rat by inoculating MT-R10. Organoid structures consist of neoplastic cells proliferating around vascular channels and are separated by necrotic tissues. HE, x 60.

Fig. 43. Tumor induced in a rat by inoculating

MT-R10. Trabecular structures consisting of thick cords of neoplastic cells are seen. HE, x 140.

Fig. 44. Tumor induced in a rat by inoculating MT-R10. Neoplastic cells reacted strongly for alkaline phosphatase. Naphthol AS method, x 140.

Fig. 45. Tumor induced in a rat by inoculating MT-R10. Infiltrating macrophages (arrows) are positive for nonspecific esterase, while neoplastic cells are negative. Alpha-naphthyl acetate method, x 180.

Fig. 46. Tumor induced in a rat by inoculating MT-R10. Neoplastic cells do not react to anti-rat monocytes/macrophages monoclonal antibody, whereas infiltrating macrophages (arrows) react positively. Indirect immunoperoxidase method, counterstained with hematoxylin, x 180.

Fig. 47. Tumor induced in a rat by inoculating MT-R10. Mature bone-tissue is accompanied by osteoids and osteoblasts. HE, x 120.

Fig. 48. Metastatic lesion in the lung of a rat inoculated subcutaneously with MT-R10. The tumor consists of small, round, undifferentiated cells. HE, x 60.

Fig. 49. Cloned cell line MT-7 consisting of round or polygonal cells with a round nucleus. HE, x 600.

Fig. 50. Cloned cell line MT-8 consisting of elongated cells with a fusiform nucleus. HE, x 600.

Fig. 51. Cloned cell line MT-9 consisting of large, round cells with the abundant cytoplasm and a lobulated nucleus. HE, x 600.

Fig. 52. Cloned cell line MT-10 consisting of dendritic cells with a few elongated cell processes. HE, x 600.

Fig. 53. Electron micrograph of MT-7 cells showing histiocytic appearances with numerous surface folds and many lysosomes in their cytoplasm. x 3,500.

Fig. 54. Electron micrograph of a part of an MT-10 cell showing a histiocytic appearance with many

lysosomes in its cytoplasm. x 9,000.

Fig. 55. Electron micrograph of MT-9 cells. The cells contain well-developed dilated rough-surfaced endoplasmic reticulum, many small lysosomes, and microfilaments (arrow) in their cytoplasm. x 7,000.

Fig. 56. Electron micrograph of a portion of an MT-9 cell showing microfilaments (arrow) in its cytoplasm. x 9,000.

Fig. 57. Electron micrograph of MT-8 cells. The cells have scant organelles, a small number of lysosomes, numerous free ribosomes, and glycogen granules in their cytoplasm. x 6,000.

Fig. 58. Electron micrograph of MT-8 cells. The cells have poorly developed cytoplasmic organelles and a small number of lysosomes. x 6,000.

Fig. 59. MT-7 cells react strongly for acid phosphatase. Gomori's method, x 700.

Fig. 60. MT-10 cells contain coarse intracytoplasmic

granules positive to anti-rat monocytes/macrophages monoclonal antibody. Indirect immunoperoxidase staining, counterstained with hematoxylin, x 700.

Fig. 61. MT-9 cells react positively for alkaline phosphatase. Naphthol AS method, x 600.

Fig. 62. Two MT-10 cells exhibit rosette formation for Fc-receptor. x 500.

Fig. 63. A pleomorphic type tumor induced in a rat by inoculating MT-7. The tumor consists of pleomorphic, round cells, and a small amount of collagenic fibers. HE, x 250.

Fig. 64. A myxoid type tumor induced in a rat by inoculating MT-10. The tumor consists of loosely arranged neoplastic cells. HE, x 180.

Fig. 65. A myxoid area of a tumor induced in a rat by inoculating MT-10. Giant cells contain hyalin globules staining red with PAS and resistant to diastase digestion. PAS stain, x 250.

Fig. 66. A myxoid area of a tumor induced in a rat by inoculating MT-10. Cells containing lipid droplets in their cytoplasm are seen. Oil red O, x 250.

Fig. 67. A storiform type tumor induced in a rat by inoculating MT-9. The tumor consists of round and elongated cells and a large amount of collagenic fibers. HE, x 200.

Fig. 68. A spindle-cell type tumor induced in a rat by inoculating MT-8. The tumor consists of spindle or fusiform cells arranged in an interlocking pattern. HE, x 200.

Fig. 69. A storiform type tumor induced in a rat by inoculating MT-9. Cells positive to anti-rat monocytes/macrophages monoclonal antibody are seen. Indirect immunoperoxidase staining, counterstained with hematoxylin, x 400.

Fig. 70. A spindle-cell type tumor induced in a rat by inoculating MT-8. Neoplastic cells are negative to anti-rat monocytes/macrophages monoclonal antibody, while infiltrating macrophages are positive to the

antibody (arrows). Indirect immunoperoxidase staining, counterstained with hematoxylin, x 300.

Fig. 71. A pleomorphic type tumor induced in a rat by inoculating MT-7. Cells positive for lysozyme (arrows) are present in the tumor. PAP method, counterstained with hematoxylin, x 300.

Fig. 72. A spindle-cell type tumor induced in a rat by transplantation of MT-8. Organoid structures consisting of neoplastic cells proliferating around vascular channels are shown. HE, x 80.

Fig. 73. A tumor induced in a rat by transplantation of MT-10. Neoplastic cells react strongly for alkaline phosphatase. Naphthol AS method, x 230.

Fig. 74. Portion of osseous tissue in a spindle-cell area of a tumor induced in a rat by transplantation of MT-8. The tumor consists of osteoids, osteoblastic cells, and undifferentiated cells. HE, x 280.

Fig. 1

Fig. 2

Fig. 3


G-7-29(8)

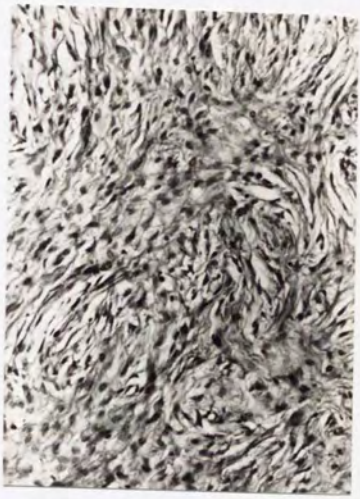

Fig. 4

Fig. 5

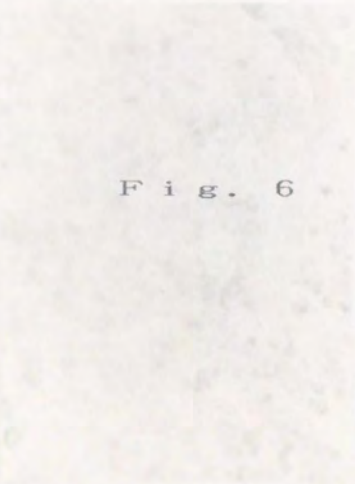

Fig. 6

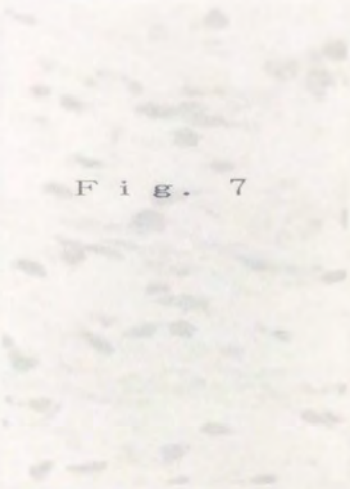

Fig. 7

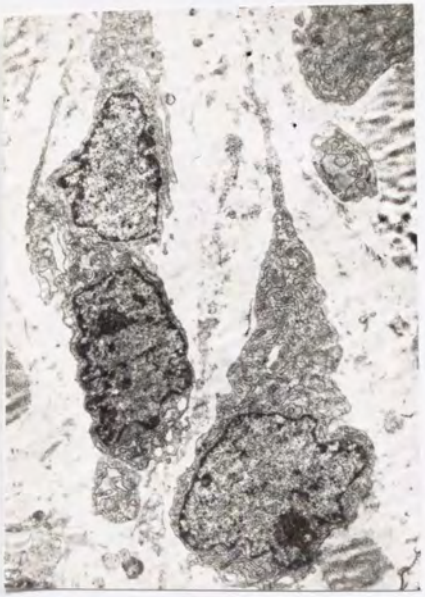


H
H
F

Fig. 8

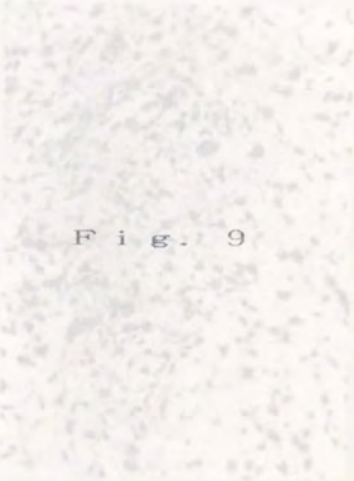

Fig. 9

Fig. 10

Fig. 11

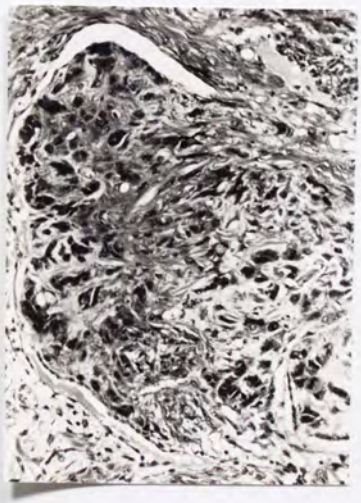

Fig. 12

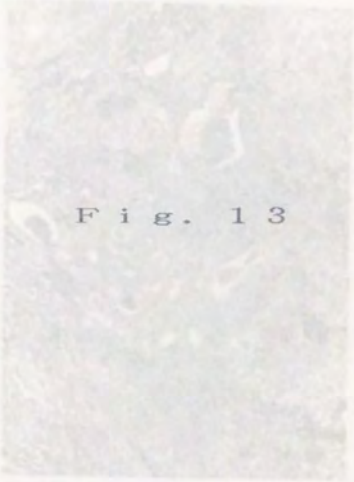

Fig. 13

Fig. 14

Fig. 15

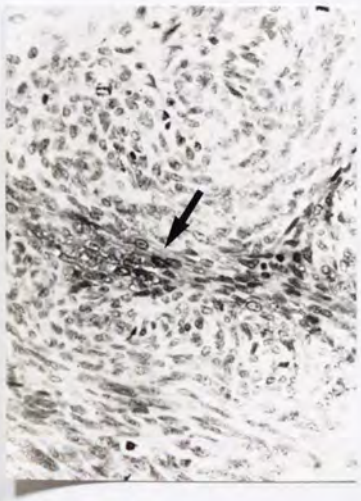

Fig. 16

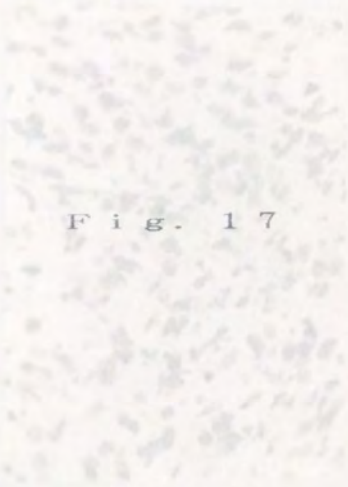

Fig. 17

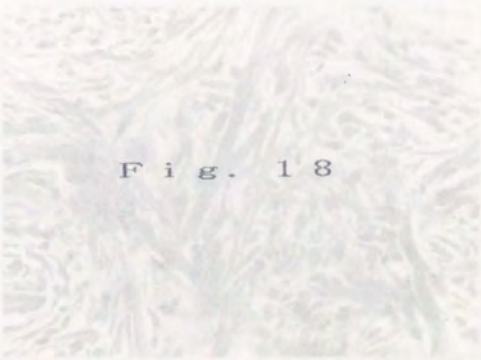

Fig. 18


G-8-A

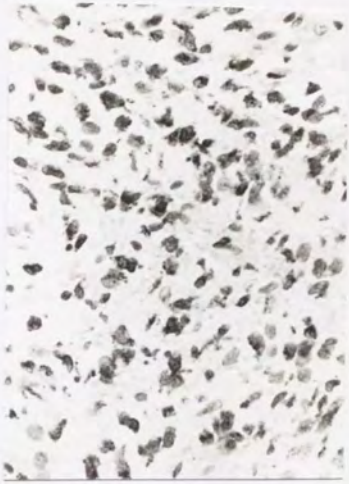

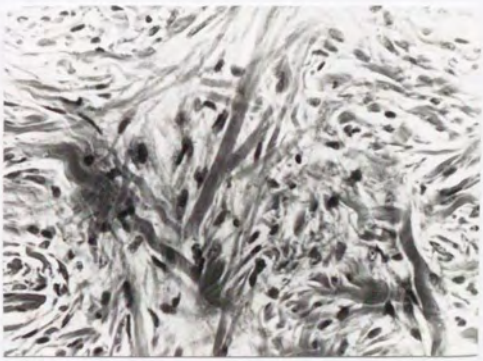

Fig. 19

Fig. 20

Fig. 21

Fig. 22

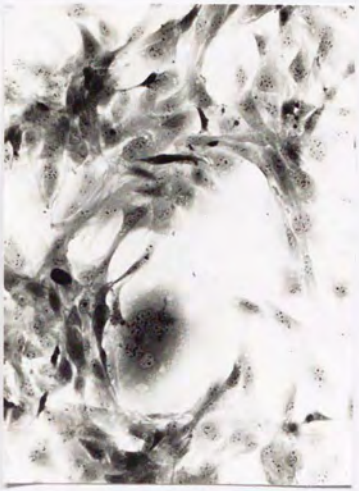

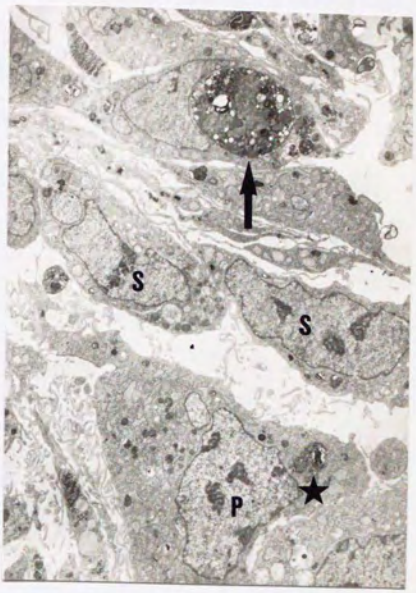
S
S
P

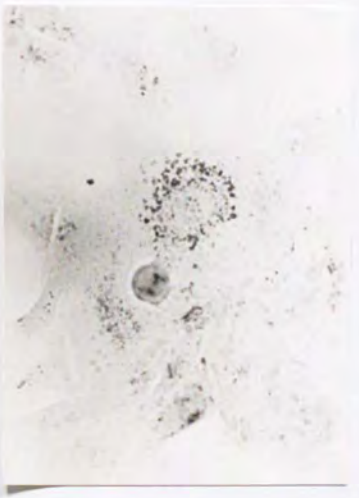

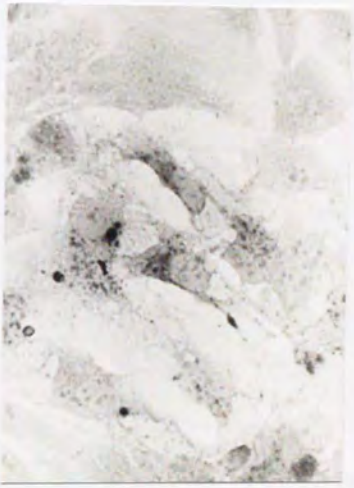

Fig. 23

Fig. 24

Fig. 25

Fig. 26

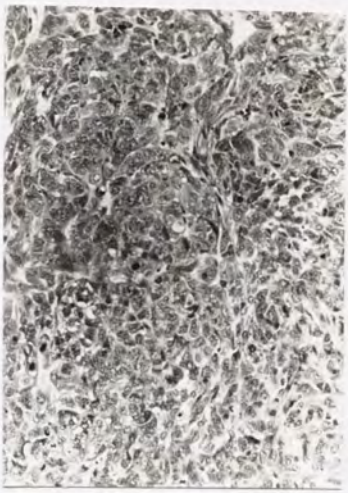

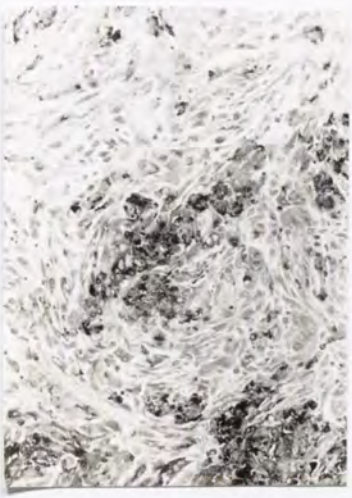

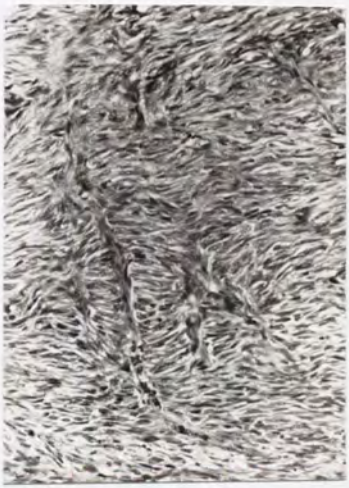

Fig. 27

Fig. 28

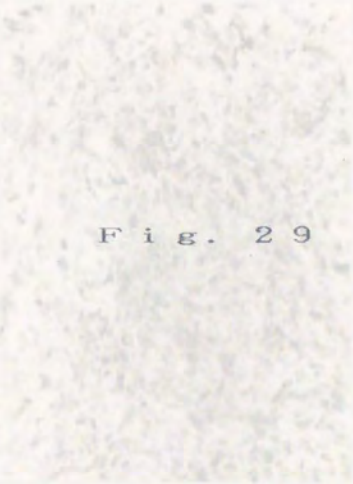

Fig. 29

Fig. 30

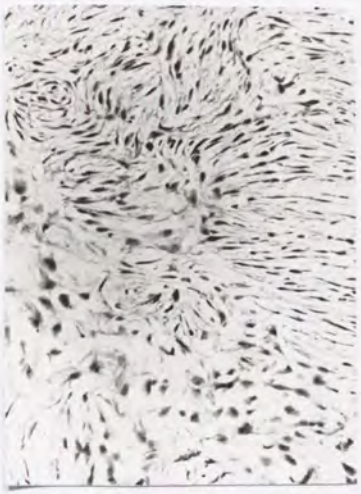

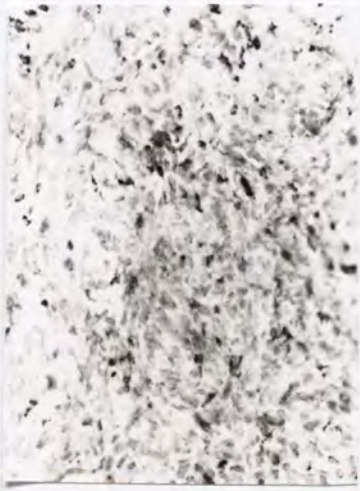

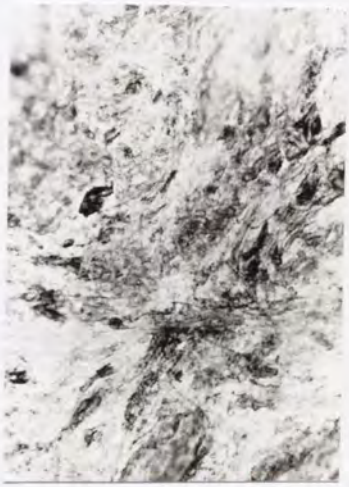

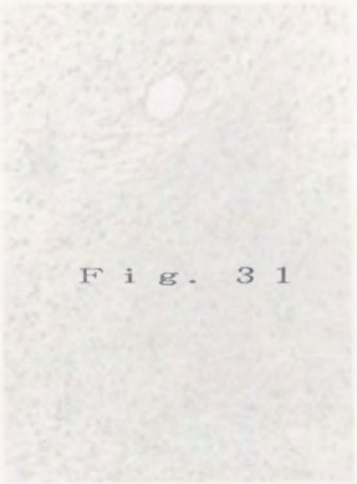

Fig. 31

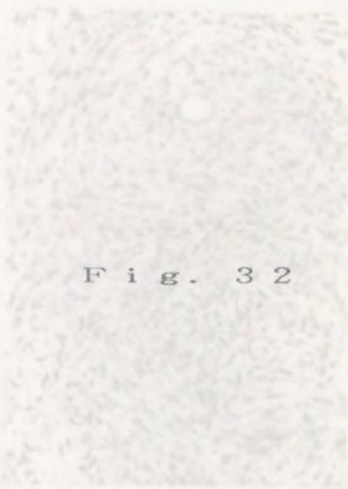

Fig. 32

Fig. 33

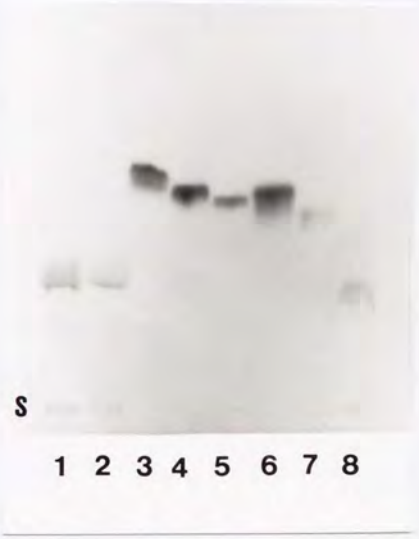
S
1 2 3 4 5 6 7 8

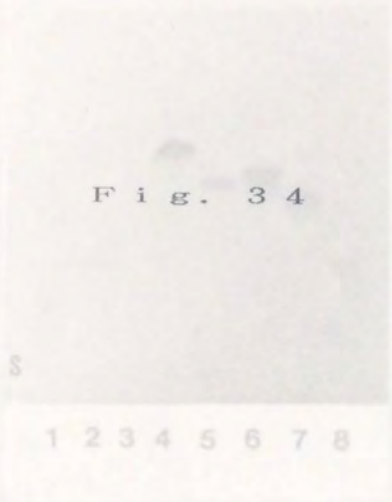

Fig. 34

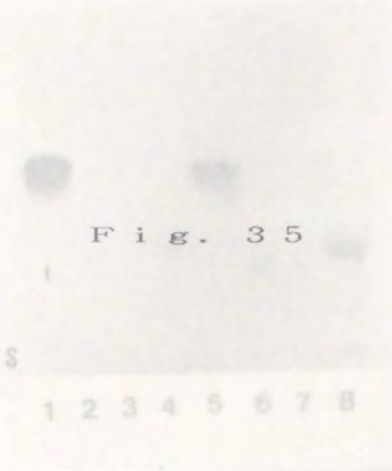

Fig. 35

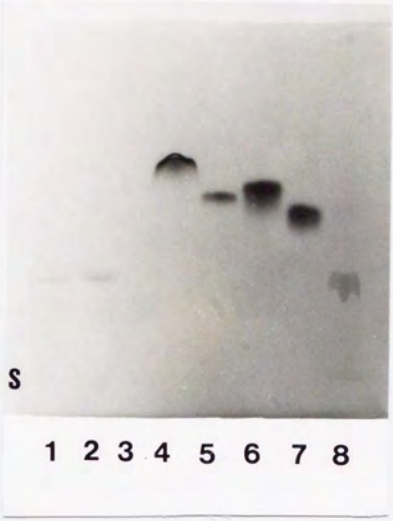
S
1 2 3 4 5 6 7 8

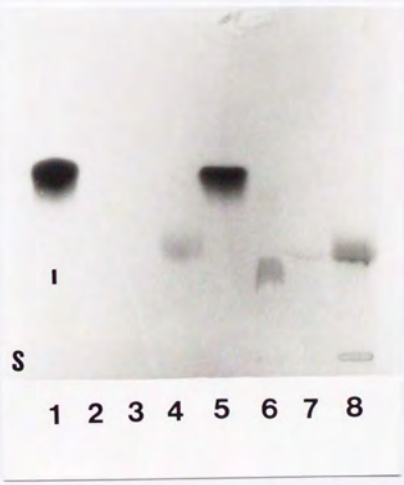
I
S
1 2 3 4 5 6 7 8

Fig. 36

Fig. 37

Fig. 38

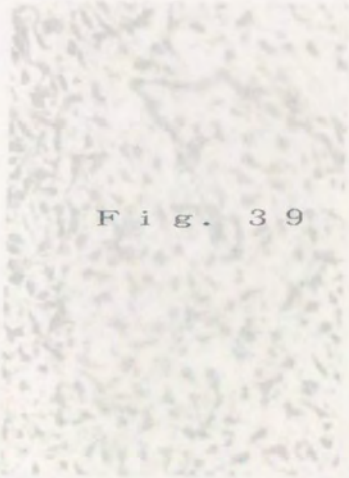

Fig. 39

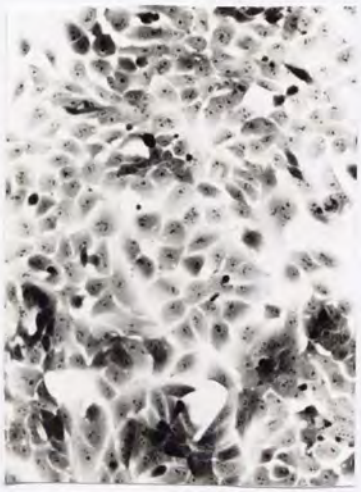

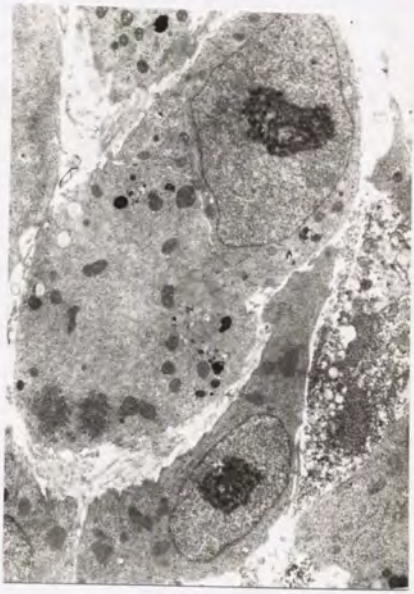

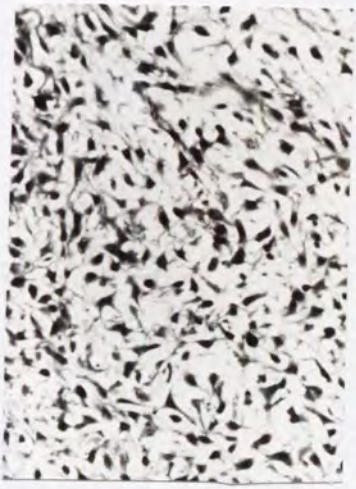

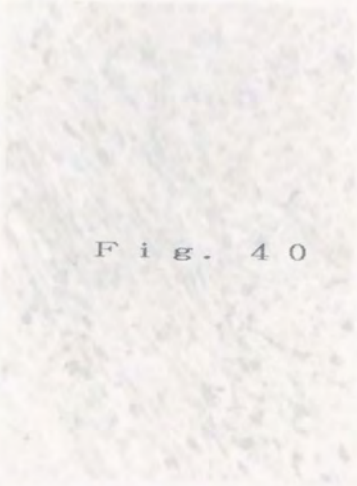

Fig. 40

Fig. 41

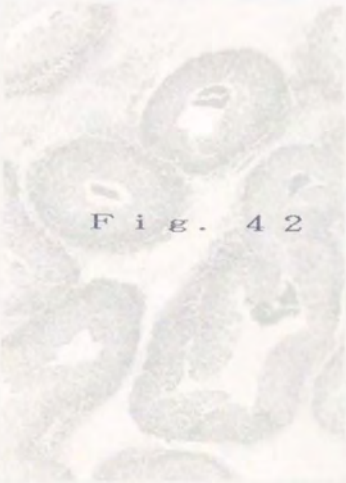

Fig. 42

Fig. 43

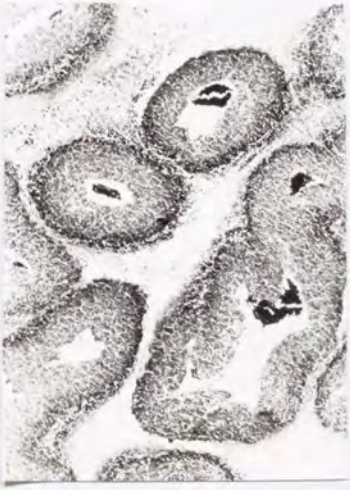

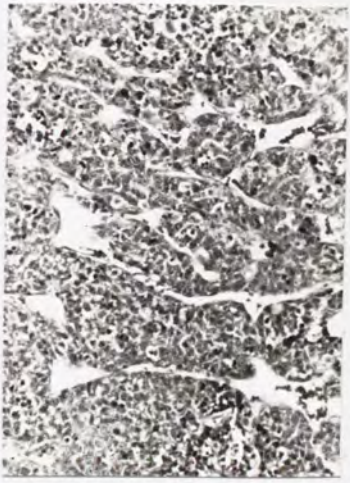

Fig. 44

Fig. 45

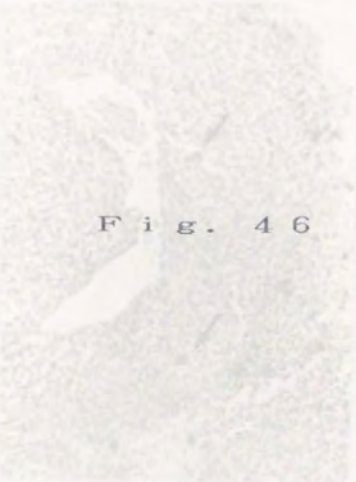

Fig. 46

Fig. 47

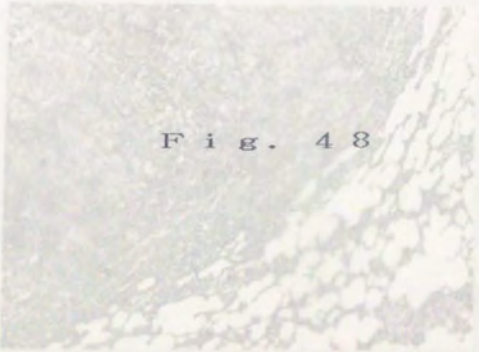

Fig. 48

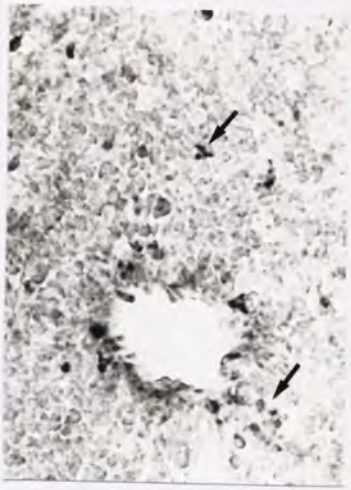

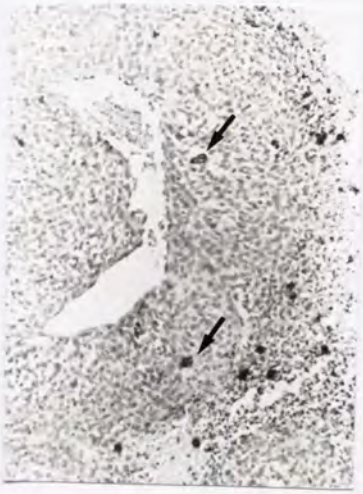

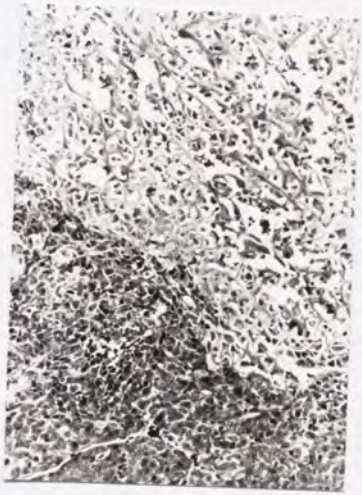

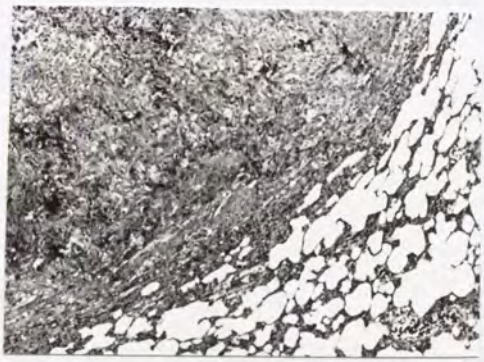

Fig. 49

Fig. 50

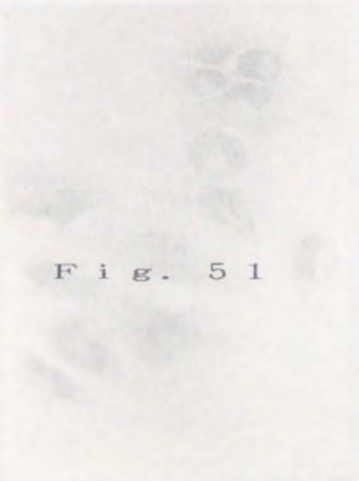

Fig. 51

Fig. 52

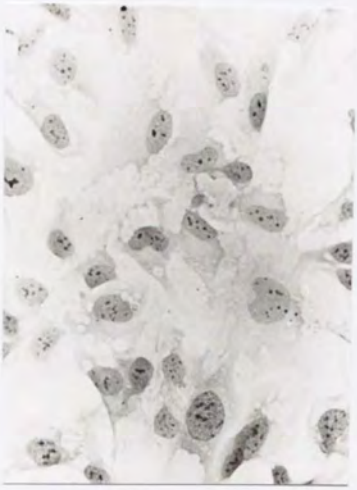

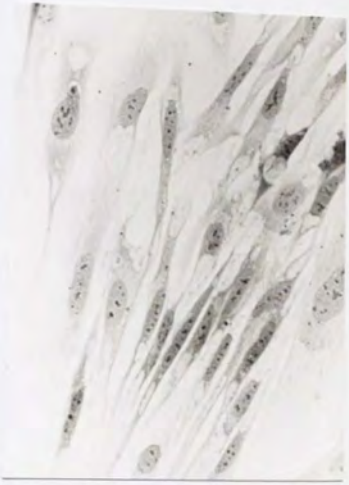

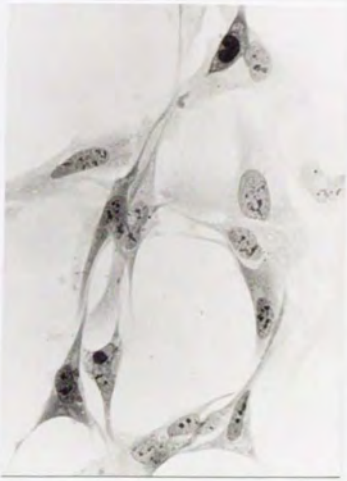

Fig. 53

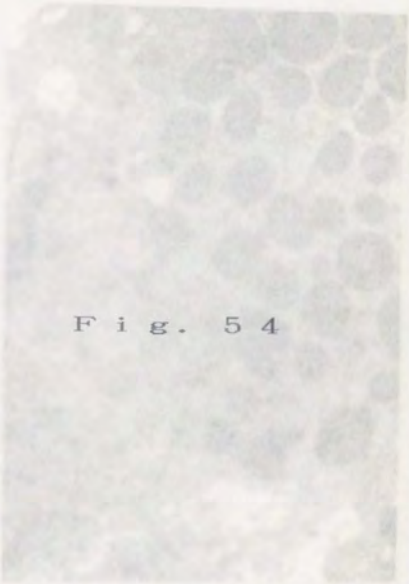

Fig. 54

Fig. 55

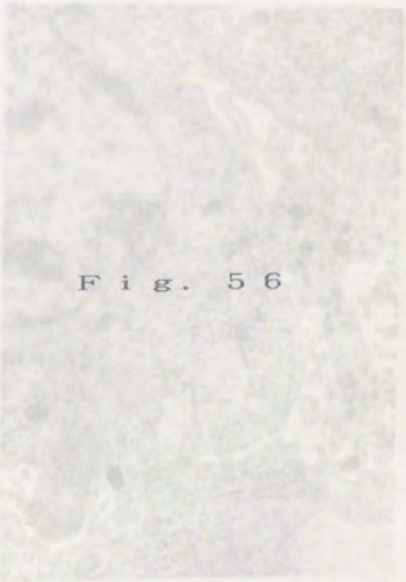

Fig. 56

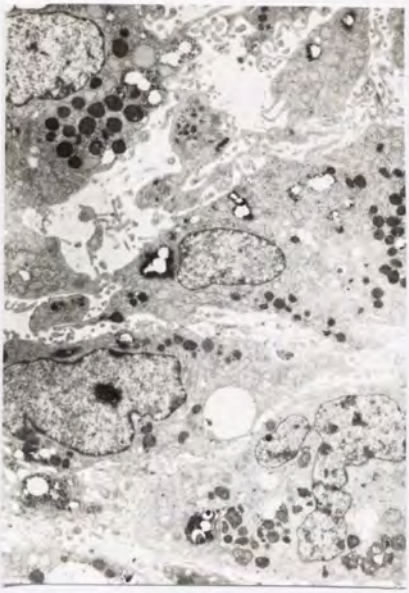

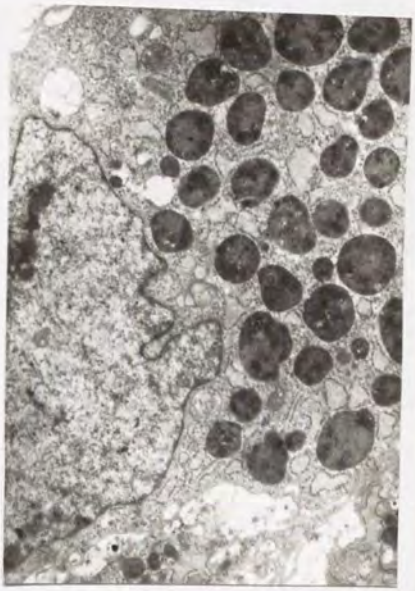

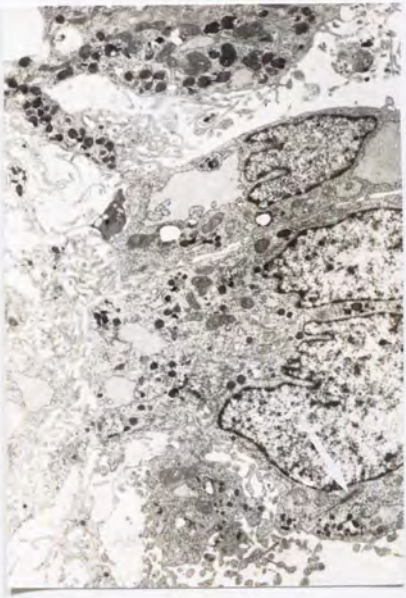

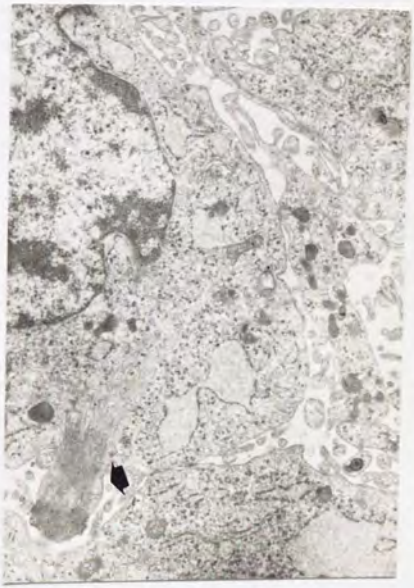

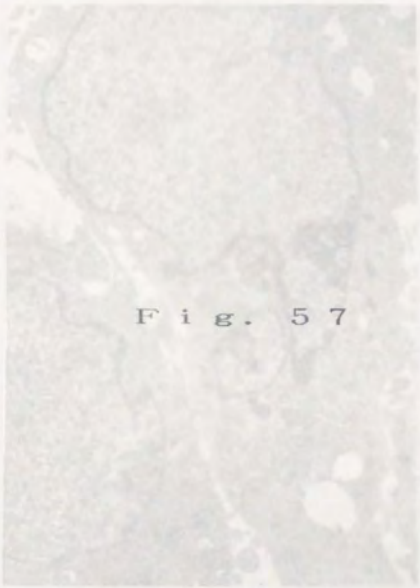

Fig. 57

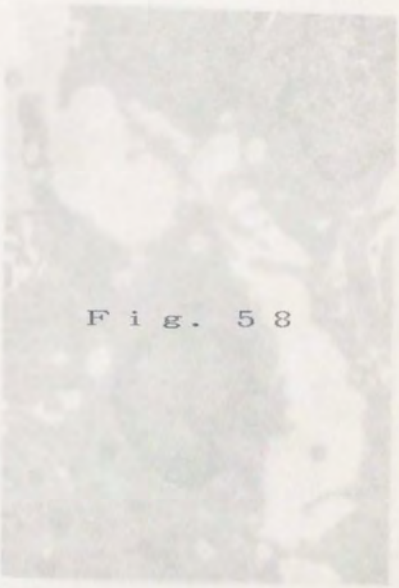

Fig. 58

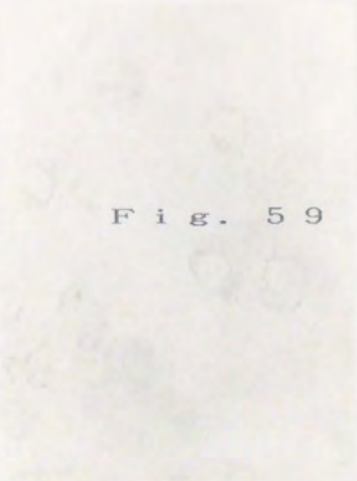

Fig. 59

Fig. 60

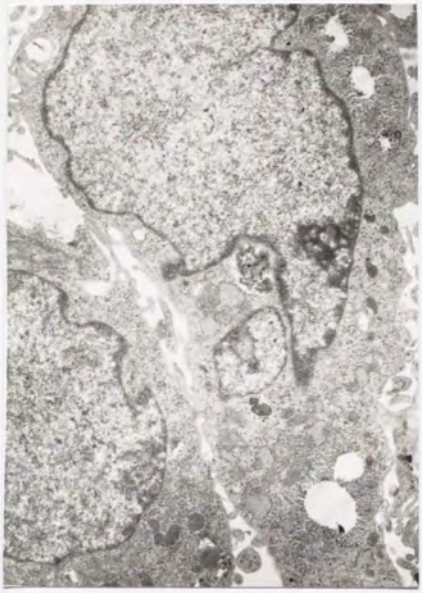

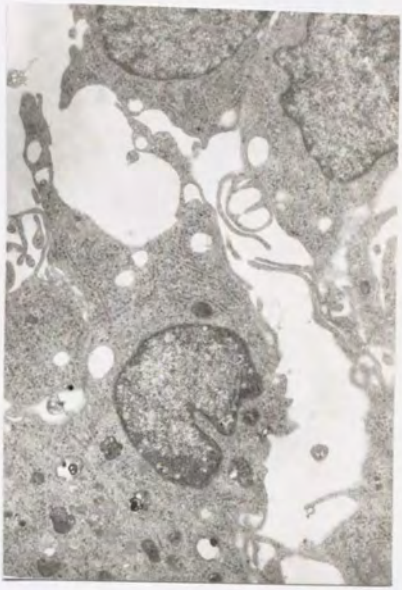

Fig. 61

Fig. 62

Fig. 63

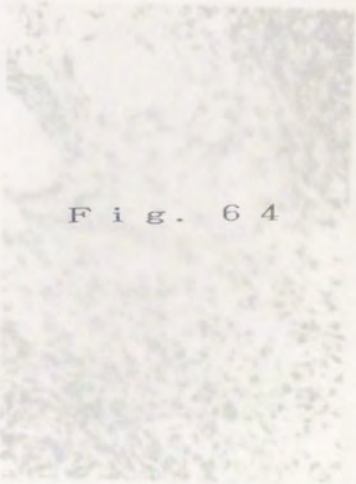

Fig. 64

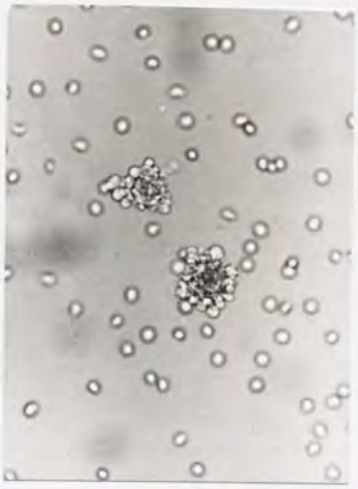

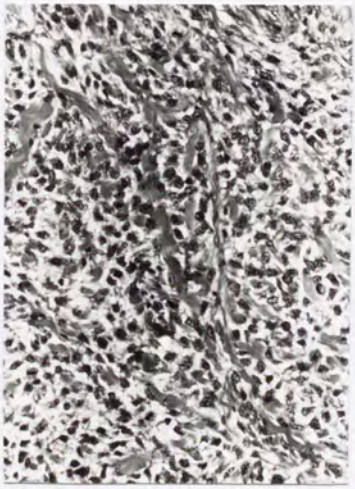

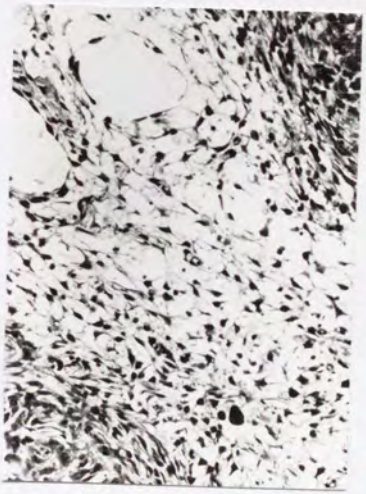

Fig. 65

Fig. 66

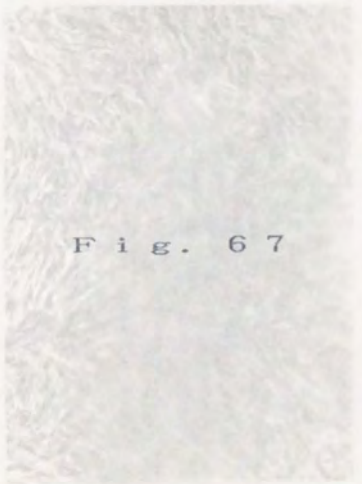

Fig. 67

Fig. 68

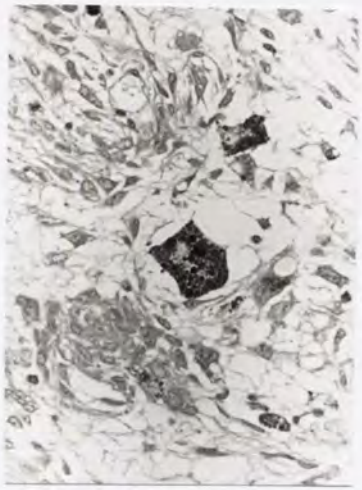

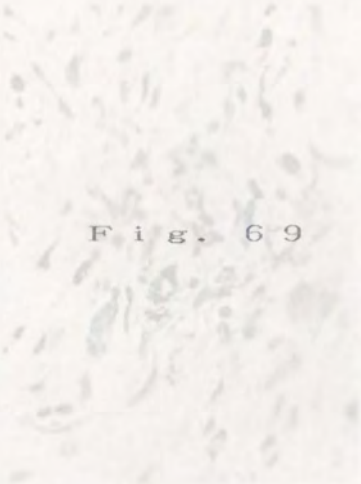

Fig. 69

Fig. 70

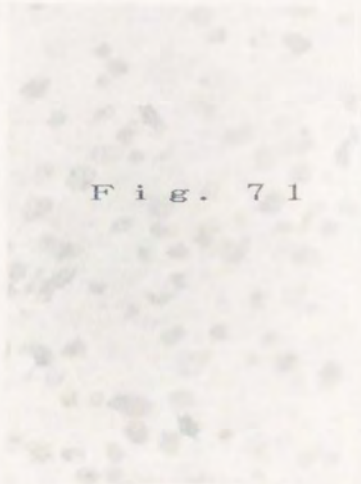

Fig. 71

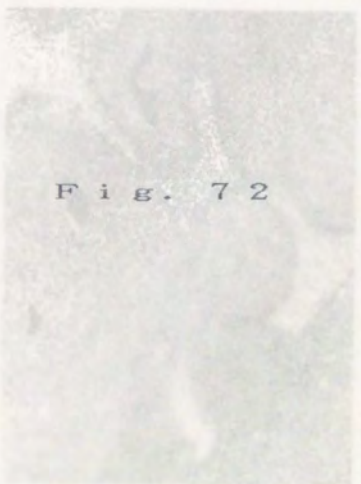

Fig. 72

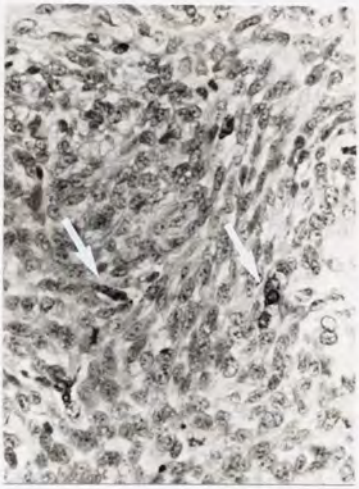

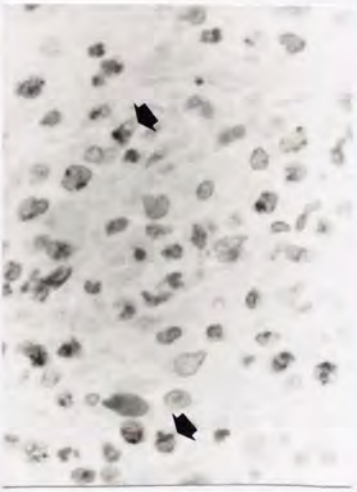

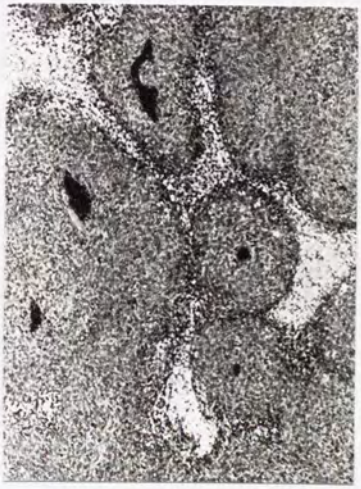

Fig. 73

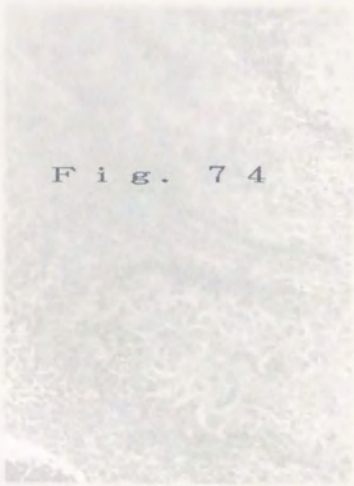

Fig. 74

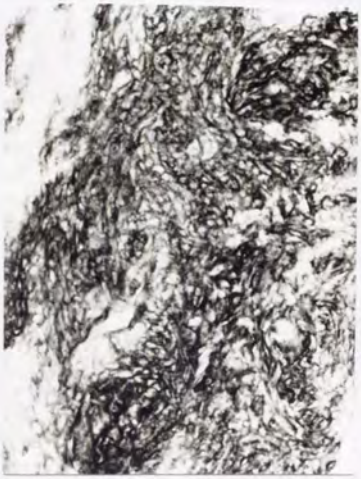

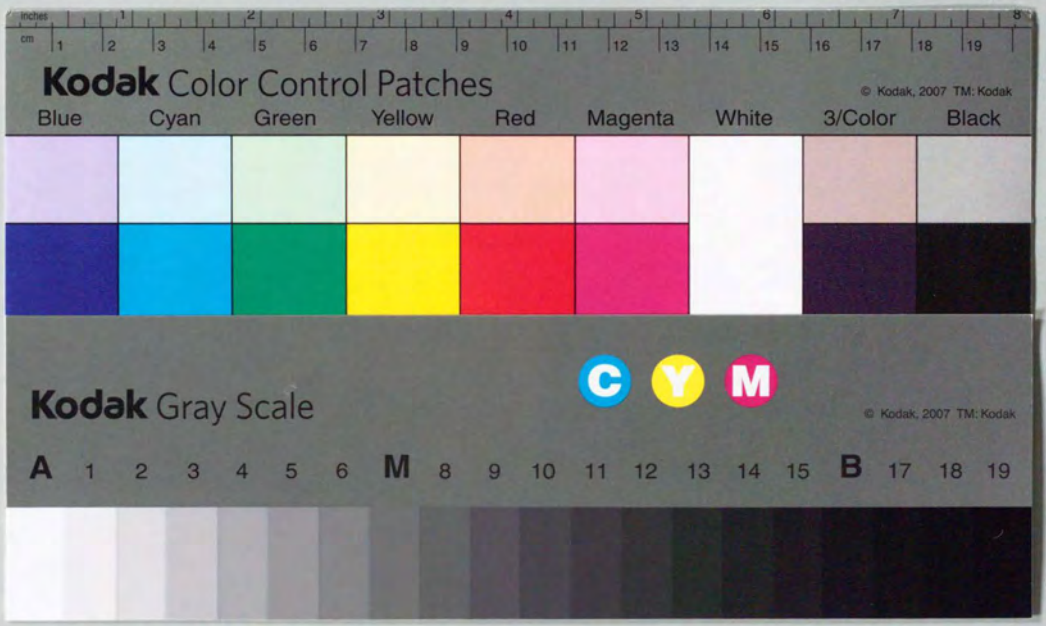
inches
cm
Kodak Color Control Patches
© Kodak, 2007 TM: Kodak
Blue
Cyan
Green
Yellow
Red
Magenta
White
3/Color
Black
Kodak Gray Scale
C
Y
M
© Kodak, 2007 TM: Kodak
A 1 2 3 4 5 6 M 8 9 10 11 12 13 14 15 B 17 18 19